

Paleozoic and Mesozoic Basement Magmatisms of Eastern Qaidam Basin, Northern Qinghai-Tibet Plateau: LA-ICP-MS Zircon U-Pb Geochronology and its Geological Significance

CHEN Xuanhua^{1,2,*}, George GEHRELS³, YIN An⁴, LI Li^{1,2} and JIANG Rongbao^{1,2}

1 *Key Laboratory of Neotectonic Movement and Geohazard, Ministry of Land and Resources, Beijing 100081, China*

2 *Institute of Geomechanics, Chinese Academy of Geological Sciences, Beijing 100081, China*

3 *Department of Geosciences, University of Arizona, Tucson, AZ 85721, USA*

4 *Department of Earth and Space Sciences, University of California, Los Angeles, CA 90095-1567, USA*

Abstract: The eastern margin of the Qaidam Basin lies in the key tectonic location connecting the Qinling, Qilian and East Kunlun orogens. The paper presents an investigation and analysis of the geologic structures of the area and LA-ICP MS zircon U-Pb dating of Paleozoic and Mesozoic magmatisms of granitoids in the basement of the eastern Qaidam Basin on the basis of 16 granitoid samples collected from the South Qilian Mountains, the Qaidam Basin basement and the East Kunlun Mountains. According to the results in this paper, the basement of the basin, from the northern margin of the Qaidam Basin to the East Kunlun Mountains, has experienced at least three periods of intrusive activities of granitoids since the Early Paleozoic, i.e. the magmatisms occurring in the Late Cambrian (493.1±4.9 Ma), the Silurian (422.9±8.0 Ma-420.4±4.6 Ma) and the Late Permian-Middle Triassic (257.8±4.0 Ma-228.8±1.5 Ma), respectively. Among them, the Late Permian - Middle Triassic granitoids form the main components of the basement of the basin. The statistics of dated zircons in this paper shows the intrusive magmatic activities in the basement of the basin have three peak ages of 244 Ma (main), 418 Ma, and 493 Ma respectively. The dating results reveal that the Early Paleozoic magmatism of granitoids mainly occurred on the northern margin of the Qaidam Basin and the southern margin of the Qilian Mountains, with only weak indications in the East Kunlun Mountains. However, the distribution of Permo-Triassic (P-T) granitoids occupied across the whole basement of the eastern Qaidam Basin from the southern margin of the Qilian Mountains to the East Kunlun Mountains. An integrated analysis of the age distribution of P-T granitoids in the Qaidam Basin and its surrounding mountains shows that the earliest P-T magmatism (293.6-270 Ma) occurred in the northwestern part of the basin and expanded eastwards and southwards, resulting in the P-T intrusive magmatism that ran through the whole basin basement. As the Cenozoic basement thrust system developed in the eastern Qaidam Basin, the nearly N-S-trending shortening and deformation in the basement of the basin tended to intensify from west to east, which went contrary to the distribution trend of N-S-trending shortening and deformation in the Cenozoic cover of the basin, reflecting that there was a transformation of shortening and thickening of Cenozoic crust between the eastern and western parts of the Qaidam Basin, i.e., the crustal shortening of eastern Qaidam was dominated by the basement deformation (triggered at the middle and lower crust), whereas that of western Qaidam was mainly by folding and thrusting of the sedimentary cover (the upper crust).

Key words: LA-ICP MS zircon U-Pb dating, thrust fault system, crust shortening and deformation, Paleozoic and Mesozoic magmatism, Qinling-Qilian-Kunlun joint zone, Qaidam Basin

1 Introduction

The eastern margin of the Qaidam Basin (Yin et al.,

* Corresponding author. E-mail: xhchen@cags.ac.cn

2007, 2008a, b) lies at the intersection of the Early Mesozoic Qinling (Jin et al., 2005; Qin et al., 2009), Early Paleozoic Qilian (Gehrels et al., 2003a) and Late Paleozoic – Early Mesozoic East Kunlun orogens (Mo et

al., 2007) which are closely related in space (Fig. 1). It is formed by a series of NW- to WNW-trending mountain chains such as the Wahong, Ela, Hacipu, Senmucike, South Xiangjia and Buerhanbuda mountains, being a part of basement upwarping in the eastern Qaidam Basin that received denudation (Chen et al., 2010). Therefore, it is a key "bridge" joining the Qinling, Qilian and Kunlun orogens, and a key area for studies of the evolution of the East Tethys Ocean (Mo et al., 2007) and the basement features of the Qaidam Basin (Liu and Gao, 1998). Meanwhile, being controlled by the thrust system (Jiang et al., 2008) and the dextral Wenquan fault zone (Wang and Burchfiel, 2004) in the area, the eastern margin of the Qaidam Basin underwent differential elevation-subsidence and denudation in the Cenozoic, which, together with the sediment-receiving Qaidam Basin, formed a coupled basin-mountain tectonic system (Chen et al., 2010).

The Neoproterozoic and Early Paleozoic magmatisms are not popular in the eastern margin of the basin. Mattinson et al. (2006, 2007) reported Mesoproterozoic granitic orthogneiss and Neoproterozoic granites in North Qaidam HP/UHP terrane. Wu C. et al. (2004a) reported an Early Paleozoic Yematan granite in the North Qaidam ultrahigh-pressure zone, which lies at ~40 km north of Dulan, consisting mainly of granodiorites, monzonitic granites and biotite granites, with zircon SHRIMP U-Pb age of 397 ± 3 Ma for granodiorite (shown in Fig. 1).

The Late Paleozoic – Early Mesozoic magmatism was of large scale and wide distribution, with its early stage dominated by intrusion of intermediate-acid rocks such as gray-white medium- to coarse-grained adamellites and granodiorites, and flesh-red porphyritic granites of the Paleo-Tethyan orogeny in the Permian - Middle Triassic (Chen et al., 2011a), and the late stage of mainly centralized continental volcanic eruption with volcanic breccias and volcanic agglomerates well developed in the Late Triassic (Chen et al., 2010). Liu et al. (2004) reported nearly identical SHRIMP II U-Pb ages of 242 ± 6 Ma, 239 ± 6 Ma and 241 ± 5 Ma (shown in Fig. 1) for granodiorite (host rock), bojite and melanocratic microgranular enclave (MME, as shown in Fig. 2) from eastern East Kunlun Mountains, respectively.

This paper presents an investigation of the features of geologic structures in the eastern Qaidam Basin and an analysis of the ages and stages of intrusive magmatisms in its basement on the basis of LA-ICP MS zircon U-Pb dating, providing the chronological base for the two time series of P-T granitoids and lithochemical trends of anti-Bowen's reaction series reported by Chen et al. (2011a). In combination with the zircon U-Pb ages provided by previous researches, the distribution and activity patterns of magmatisms in the basin basement

during the Permo-Triassic (P-T) time is suggested, and the pattern of the shortening and deformation of the basement in the Cenozoic is further discussed.

2 Geological Setting of the Eastern Margin of Qaidam Basin

According to previous works and our observations in the field, the geological setting of the eastern margin of the Qaidam Basin is described as follows.

2.1 Metamorphic and sedimentary basement of eastern Qaidam Basin

The metamorphic crystalline basement of the Proterozoic Shaliuhe Group occurs as faulted block between Dulan and Wulan towns in the eastern margin of the Qaidam Basin (shown in Fig. 1; QBGM, 1991; Zhang et al., 2005). The rocks are dominated by two-mica plagiogneiss, biotite plagiogneiss, plagioclase-rich amphibolite and marble, containing eclogite lenses (Yang et al., 2002; Xu et al., 2003). Caused by the combined action of the Dulan detachment fault (DDF; Fig. 1) and the Dulan thrust (DT) which belong to the E-W-trending tectonic system, the ultrahigh-pressure metamorphic eclogite-bearing gneisses (Yang et al., 2002; Xu et al., 2003) in the area uplifted to the surface. This process is similar to that in the Lüliangshan and Xitieshan areas, northern Qaidam Basin (Meng et al., 2005; Menold et al., 2009).

The sedimentary basement of eastern Qaidam Basin consists of Lower Paleozoic Asizha Group, Upper Devonian Maoniushan Formation, Carboniferous, and Permian System. The Lower Paleozoic Asizha Group is a suite of pyroclastic rocks of littoral-neritic facies. The Upper Devonian Maoniushan Formation is a suite of typical continental volcanic formation and molasse formation, with the bottom consisting of polymictic conglomerates, fining upward with increasing composition of andesitic volcanic rocks, and the top dominated by feldspar quartz sandstones. The Lower Carboniferous is composed of three rock series: continental clastic rocks, littoral-neritic carbonate rocks and paralic carbonate rocks intercalated with clastic rocks in ascending order. For the Upper Carboniferous, the lower part consists of gravel-bearing grit stones, volcanic breccias intercalated with dacites and carbonate rocks, and the upper part of calcareous siltstones, carbonaceous slates, rheolites and dacites. The Permian System is formed by a suite of neritic clastic rocks, carbonate rocks and volcanic formations, and the rocks are dominated by gray-white quartz sandstones, sandy slates and tuffaceous slates, with minor limestones, basalts and rheolites. The Triassic

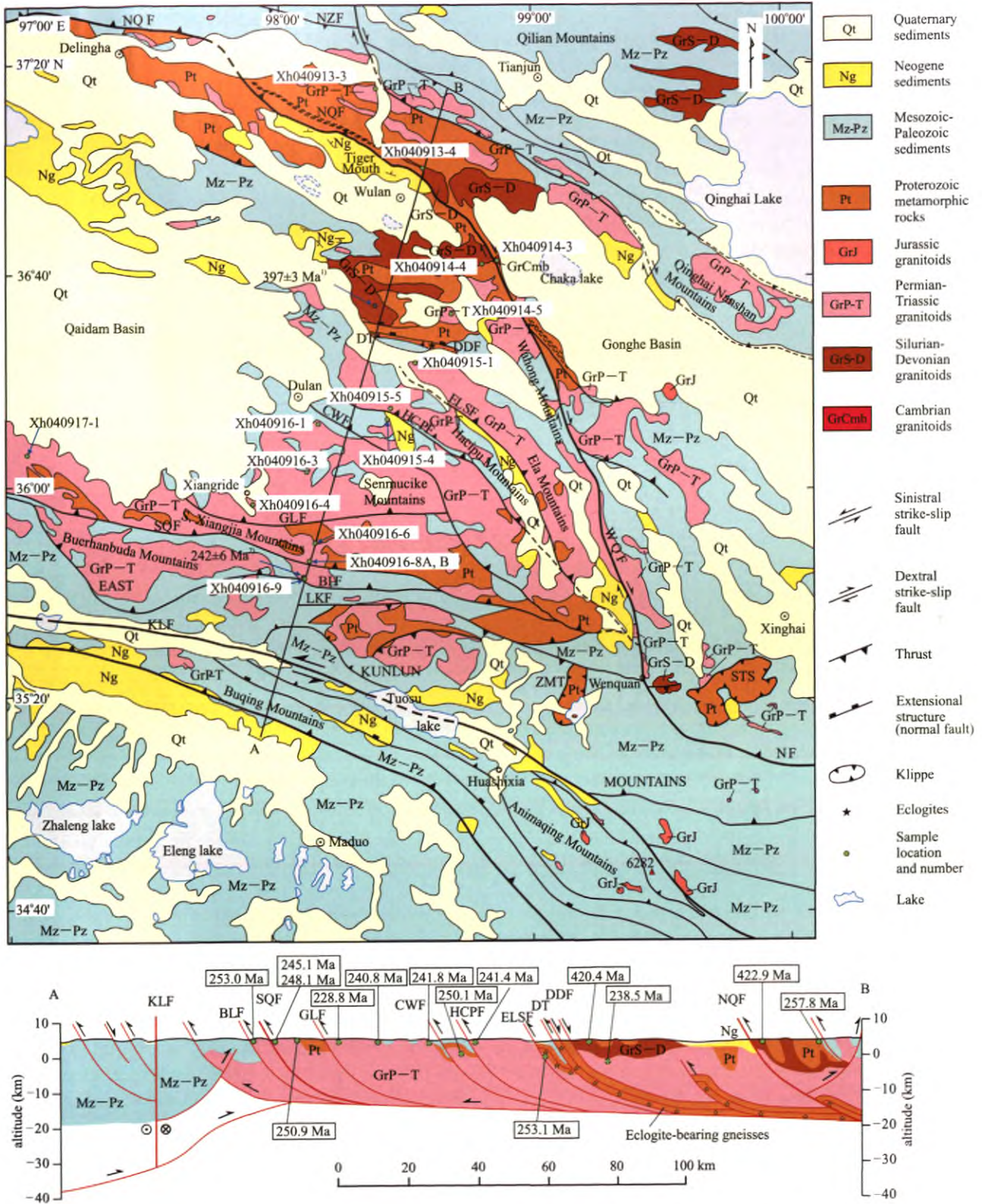


Fig. 1. A sketched map of geological structures in the eastern margin of the Qaidam Basin (modified from Jiang et al., 2008 and Chen et al., 2011a), showing sample localities (above) and LA-ICP MS zircon U-Pb ages distribution on the section (below). Unit of age: Ma. U-Pb ages from other studies are also shown: 1) Wu C. et al., 2004a; 2) Liu C. et al., 2004. WQF, the Wenquan fault (also called the Wahongshan fault); NZF, North Zongwulongshan fault; NQF, North Qaidam fault; ELSEF, Elashan fault; HCPF, Hachipu fault; CWF, Chahanwusu fault; GLF, Gouli fault; SQF, South Qaidam fault; BLF, Boluoer fault; LKF, Longwakalu fault; DDF, Dulan detachment fault; DT, Dulan thrust; NF, Nanmutang fault. STS, Saishitangshan klippe; ZMT, Zuimatan klippe.

System is very thick with complex rock formations: the Lower, composed of conglomerates, feldspar sandstones, tuffs, andesites and limestones; the Middle, a suite of littoral-neritic clastic rocks, carbonate rocks and volcanic formation; the Upper, continental intermediate-acid volcanic lavas and volcanic clastic rocks, dominated by andesites, rhyolites and dacites, with tuffs and vitric and crystal tuffs, locally of volcanic breccias and volcanic agglomerates (QBGMR, 1991; Zhang et al., 2005).

2.2 Mesozoic and Cenozoic covers of eastern Qaidam Basin

The Mesozoic and Cenozoic covers of eastern Qaidam Basin (Zhong et al., 2004) consist mainly of Jurassic, Neogene, and Quaternary systems. The Jurassic System outcropped here is composed of thick-bedded tuffaceous conglomerates, tuffs, dacitic lavas, andesitic lavas and volcanic conglomerates, intercalated with coal seams. The Neogene System consists of a suite of piedmont-lacustrine red clastic rock formation under arid climate conditions, with lower part composed of conglomerates intercalated with gypsum beds, while the upper part of gravel-bearing sandstones, siltstones and mudstones. The widely distributed Quaternary System is about 1.4 km, consisting of glacial, pluvial, alluvial-pluvial, alluvial and eolian sediments (QBGMR, 1991; Zhang et al., 2005).

2.3 Structural geologic features of eastern margin of Qaidam Basin

The eastern margin of the Qaidam Basin is a composite part of the structural system subject to combined actions of the East Kunlun, the Qilian and the West Qinling orogeneses across the Qaidam and Gonghe basin basement (Fig. 1). The NE-dipping Eastern Qaidam thrust system and NNW-trending Wenquan (Wahongshan) fault zone (Wang and Burchfiel, 2004) developed in the Mesozoic and Cenozoic, have caused the metamorphic basement and pre-Mesozoic sedimentary basement to upwarp, thereby separating the Qaidam Basin from the Gonghe Basin (Fig. 1).

2.3.1 The Eastern Qaidam thrust system

The Eastern Qaidam thrust system lies between the North Zongwulongshan fault (NZF) on the south margin of the Qilian Mountains and the Kunlun fault (KLF) of the East Kunlun Mountains (Fig. 1). It is composed mainly of the South Qaidam fault (SQF) developed in the central East Kunlun Mountains in the south and the North Qaidam fault (NQF) in the southern margin of the Qilian Mountains in the north, as well as a series of thrusts developed in the Qaidam Basin basement in-between, which are, from north to south, the Elashan fault (ELSF),

Hacipu fault (HCPF), Chahanwusu fault (CWF; an eastward extending of the Lüliangshan-Xitieshan south fault, LXSF), and Gouli fault (GLF). The Boluoer fault (BLF) occurs on the south side of the South Qaidam fault.

Due to the faulting of the NE-dipping Cenozoic Eastern Qaidam thrust system, a number of faulted blocks and residual Cenozoic basins (including the Wulan basin at the south of NQF, the Dudaitan basin at the south of ELSF, the Yangchanggou basin at the south of HCPF, etc.) have formed in the eastern margin of the Qaidam Basin (Fig. 1). These basins are all filled with sediments of the Miocene Xiayoushashan Formation (23.8–11.2 Ma; Yin et al., 2007, 2008b), which indicates that this thrust system should have formed in the early Neogene.

The North Qaidam fault (NQF), which trends in NW and dips to the NE, is the main thrust fault of the ~800 km-long Northern Qaidam thrust system at the southeast part of the Southern Qilian Shan-Nan Shan thrust belt (Yin et al., 2008a), forming the northern Qaidam Basin as an example of the reformative foreland basin (Song et al., 2010). It thrusts the Proterozoic and Early Paleozoic volcanic rocks and P-T granites and granodiorites onto the red bed of Miocene Youshashan Formation in the Wulan basin (Fig. 1).

The Hacipu fault (HCPF, Fig. 3) lies on the south side of Hacipu Mountain ("Hacipu" means plenty of tents in Mongolian). It thrusts the Triassic Hacipushan granitoid intrusives onto the Neogene Youshashan Formation in Yingteer Yangchang valley, and formed a series of concealed thrust faults and related anticlinal folds inside the Neogene System, which are featured by an echelon distribution, showing their growth from NW to SE (Jiang et al., 2008). The similar geomorphologic feature of anticlinal mountains and valley basins indicates that the thrusting front of HCPF tends to be developed from NW to SE in the Quaternary or still active (Jiang et al., 2008).

The E-W extending South Qaidam fault (SQF, Fig. 1) over 1000 km, formerly called as the central East Kunlun fault, superposed the Qaidam Basin's basement onto the East Kunlun Mountains, resulting in the piggyback Qaidam Basin of the East Kunlun Mountains. SQF is partially developed as a low-angle thrust in the layered granodiorite batholith (Fig. 4), with a series of fractured structures filled by K-feldspar-rich granitic veins. The southward splay of SQF is the Boluoer fault (BLF) to the south (Fig. 1). Melanocratic microgranular enclaves are abundant in the hanging wall of both SQF and BLF (Fig. 2).

On the southern margin of the eastern Qaidam Basin there are some N-dipping thrusts and klippen, with a few N-thrusting faults acting as back thrusts (Fig. 1; QBGMR, 1991; Zhang et al., 2005; Chen et al., 2011b). Among

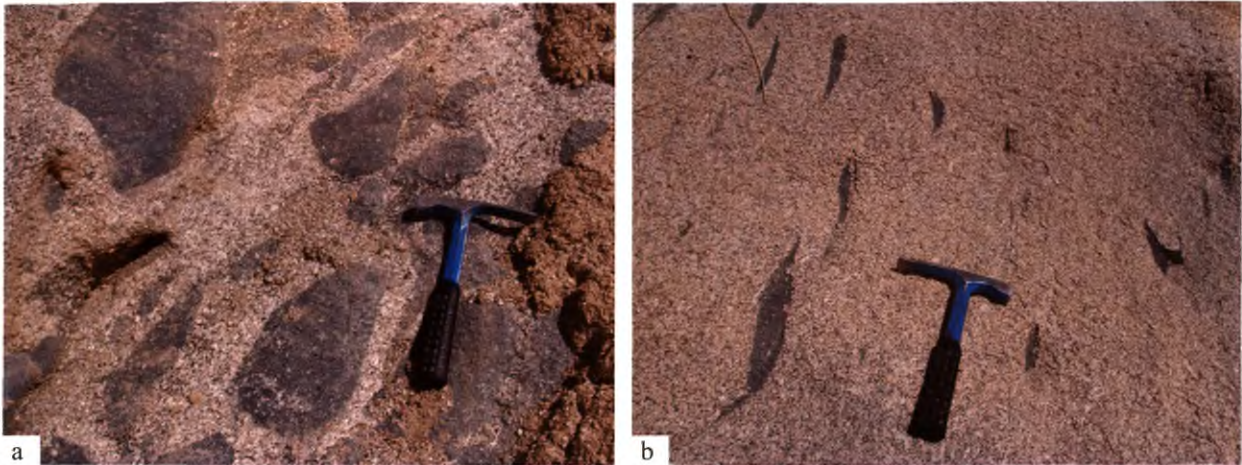


Fig. 2. Melanocratic microgranular enclaves (MMEs) in granodiorite from the hanging walls of the South Qaidam fault (a) and the Boluoer fault (b).

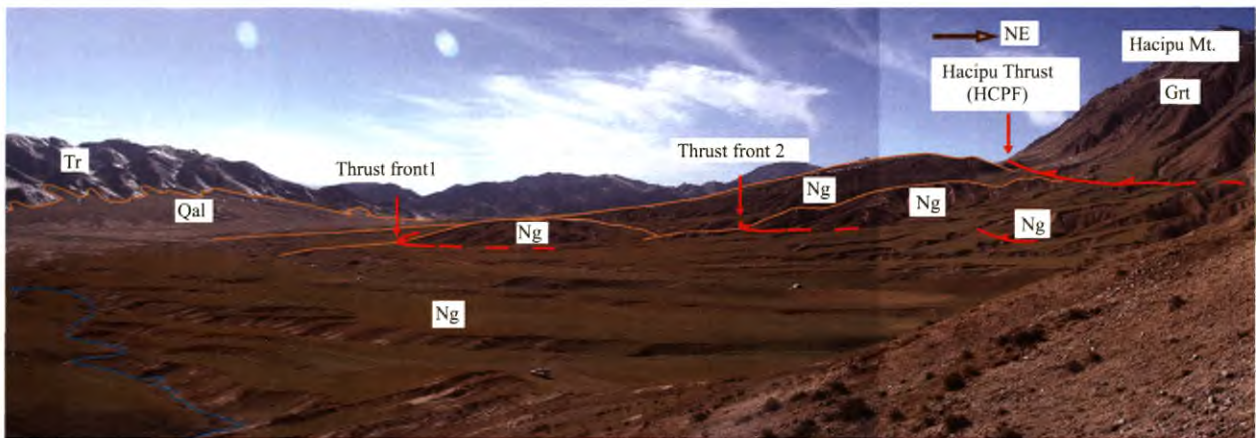


Fig. 3. Hacipu fault of the eastern Qaidam thrust fault system, showing thrust fronts. Note that, for scale, the white car in the bottom of the photo is about 3 m long.

them, the Saishitangshan (STS) and Zuimatan (ZMT) klippen are the two relatively large ones (Fig. 1; QBGMR, 1991; Zhang et al., 2005). They have superposed the Proterozoic biotite plagiogneisses and two-mica quartz slates onto flysch formations of the Permian and Triassic (dominant) (QBGMR, 1991; Zhang et al., 2005).

2.3.2 The Wenquan fault zone

The Wenquan fault zone (WQF, Fig. 1), which is also called as the Wahongshan fault zone, is the main strike-slip fault of the Wenquan right-lateral strike-slip fault system, extending NNW for over 200 km (Wang and Burchfiel, 2004; Jiang et al., 2008). It truncated the high relief ranges such as Wahong, Ela and East Kunlun Mountains at its western side and a basin (i.e. the Gonghe basin) or low hills (the West Qinling Mountains) at east. It consists of 3 to 5 faults, which are distributed in a parallel en echelon arrangement. Its north end cuts the North

Qaidam fault obliquely, and the south end cuts off the South Qaidam fault. The fault system forms the dividing boundary between the Qaidam and the Gonghe basins, and also the intersection of the East Kunlun and West Qinling mountains (Jiang et al., 2008). The Wenquan fault is considered to be an intercrustal transform fault, which merges into the WNW-trending N-dipping Nanmutang fault in the south and the N-dipping NQF in the north (Fig. 1).

Along the fault zone there are some flat valleys, fault scarps, triangular facets and warm springs in line, with frequent seismic activities. The fault zone strikes 330° - 350° in general, and most of the fault planes dip southwest with steep angles of 50° - 70° . It is dominated by brittle deformation. The main fault-compression fractured zone may have a width from ~ 50 m to >200 m, filled with gouges, ultra-cataclastic rocks, tectonic breccias and tectonic lenses (such as granodiorite blocks of various

sizes and shapes). The granitic bodies on the two sides of the southern segment of the fault zone have been obviously truncated in dextral style with apparent displacement of ~10 km.

The Wenquan fault and the sinistral Altyn Tagh fault (Yin et al., 2002; Chen Z. et al., 2002, 2004) have opposite shearing directions, hence some researchers regard them as a pair of conjugate faults, which absorb together the inseting of Qaidam Basin's rigid basement toward the Qilian Mountains from south to north (Wang and Burchfiel, 2004). However, the formation ages of these two faults differ greatly: the Altyn Tagh fault formed at ~49 Ma (Yin et al., 2002), whereas the Wenquan fault formed later than the North Qaidam fault, probably in late Miocene-early Pliocene (Wang and Burchfiel, 2004). Besides, they also vary greatly in the scale of strike-slipping: the former has a sinistral strike-slip displacement of ~500 km, while the dextral displacement of the latter is only ~20 km (Wang and Burchfiel, 2004). Thus, they formed into the conjugate shearing fault system only since the late Miocene.

2.3.3 The Gonghe Basin

It is an intermountane basin between Qinghai Nanshan Mountains and Wahong Mountains, located in the west segment of the West Qinling Indosinian fold zone. It is controlled by the Zongwulongshan-Nanshan fault in north and the Wenquan fault zone in west. The basin is ~280 km long and 30-95 km wide, with an area of $\sim 1.57 \times 10^4$ km².

The Gonghe and the eastern Qaidam basins are surprisingly similar in terms of Quaternary sedimentation, including the sedimentation environments, sediments and their thickness, stratigraphic sequences, characteristics of fossils, lithology of rocks, features of seismic reflection, tectonic states, etc (Wang and Lü, 2004).

3 U-Pb Geochronology of Intrusive Magmatism in the Eastern Margin of Qaidam Basin

3.1 Sample collection and preparation, and U-Pb geochronologic analyses of zircons

A total of 16 granitoid samples were collected from eastern margin of the Qaidam Basin, starting from the location about 18 km north of the North Qaidam fault and following the 230-km long NE-trending profile to the East Kunlun magmatic zone (see Fig. 1 for sampling locations). Lithochemical and Nd-Sr-Pb-O isotopic analyses of all these samples had been reported by Chen et al. (2011a). Zircons were extracted from these samples through a series of mineral separation procedures, including utilizing a roller crusher, heavy liquids, and a Frantz isodynamic

separator, and hand picking under the binocular microscope to select zircon grains of good crystal form, transparency and color. The zircon samples were put into epoxy resin, solidified, and then polished and ground to half size when the cores of zircons were fully exposed.

U-Pb geochronology of zircons was conducted by laser ablation multicollector inductively coupled plasma mass spectrometry (LA-MC-ICP MS) at the Arizona LaserChron Center (Gehrels et al., 2006, 2008; Johnston et al., 2009). The analyses involve ablation of zircon with a New Wave/Lambda Physik DUV193 Excimer laser (operating at a wavelength of 193 nm) using a spot diameter of 35 microns. The ablated material is carried with helium gas into the plasma source of a GV Instruments Isoprobe, which is equipped with a flight tube of sufficient width that U, Th, and Pb isotopes are measured simultaneously. All measurements are made in static mode, using Faraday detectors for ²³⁸U and ²³²Th, an ion-counting channel for ²⁰⁴Pb, and either Faraday collectors or ion counting channels for ²⁰⁸⁻²⁰⁶Pb. Ion yields are ~1 mv per ppm. Each analysis consists of one 20-second integration on peaks with the laser off (for backgrounds), 20 one-second integrations with the laser firing, and a 30 second delay to purge the previous sample and prepare for the next analysis. The ablation pit is ~15 microns in depth.

For each analysis, the errors in determining ²⁰⁶Pb/²³⁸U and ²⁰⁶Pb/²⁰⁴Pb contribute a measurement error of ~1% (at 2-sigma level) in the ²⁰⁶Pb/²³⁸U age. The errors in measurement of ²⁰⁶Pb/²⁰⁷Pb and ²⁰⁶Pb/²⁰⁴Pb also contribute ~1% (2-sigma) uncertainty in age for grains that are >1.0Ga, but are substantially larger for younger grains due to low intensity of the ²⁰⁷Pb signal. For most analyses, the cross-over in precision of ²⁰⁶Pb/²³⁸U and ²⁰⁶Pb/²⁰⁷Pb ages occurs at ~1.0Ga.

Common Pb correction is done by using the measured ²⁰⁴Pb and assuming an initial Pb composition from Stacey and Kramers (1975) (with uncertainties of 1.0 for ²⁰⁶Pb/²⁰⁴Pb and 0.3 for ²⁰⁷Pb/²⁰⁴Pb). Our measurement of ²⁰⁴Pb is unaffected by the presence of ²⁰⁴Hg because backgrounds are measured on peaks (thereby subtracting any background ²⁰⁴Hg and ²⁰⁴Pb), and because very little Hg is present in the argon gas.

Inter-element fractionation of Pb/U is generally ~20%, whereas fractionation of Pb isotopes is generally <2%. In-run analysis of fragments of a large zircon crystal (generally every fifth measurement) with known age of 564±4 Ma (2-sigma error) is used to correct for this fractionation. The uncertainty resulting from the calibration correction is generally ~1% (2-sigma) for both ²⁰⁶Pb/²⁰⁷Pb and ²⁰⁶Pb/²³⁸U ages.

3.2 U-Pb geochronological results

The tables of analytical data are too long, they are not listed here. Uncertainties shown in these tables are at the 1-sigma level, and include only measurement errors. The analyses are also shown on Pb/U concordia diagrams in the order from the oldest to the youngest (Figs. 5 and 6).

The reported ages are determined from the weighted mean (Ludwig, 2003) of the $^{206}\text{Pb}/^{238}\text{U}$ or $^{206}\text{Pb}/^{207}\text{Pb}$ ages of the concordant and overlapping analyses (Figs. 5 and 6). Analyses that are statistically excluded from the main cluster are shown in blue on these figures. Two uncertainties are reported on these plots. The smaller uncertainty (labeled "mean") is based on the scatter and precision of the set of $^{206}\text{Pb}/^{238}\text{U}$ or $^{206}\text{Pb}/^{207}\text{Pb}$ ages, weighted according to their measurement errors (shown at 1-sigma). The larger uncertainty (labeled "age"), which is the reported uncertainty of the age, is determined as the quadratic sum of the weighted mean error plus the total systematic error for the set of analyses. The systematic error, which includes contributions from the standard calibration, age of the calibration standard, composition of common Pb, and U decay constants, is generally ~1%–2% (2-sigma).

For the purpose of checking if the zircon grains to be tested are of one stage magmatic origin so that they can

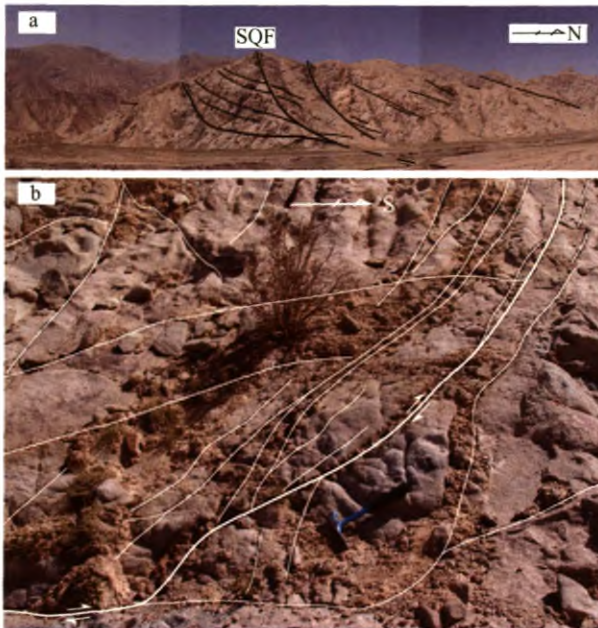


Fig. 4. Development of the South Qaidam fault within layered granodiorites in the middle-eastern segment of the East Kunlun Mountains, showing north-dip thrust.

(a) Several thrusts developed in the South Qaidam fault zone, view to west. (b) Local feature of the South Qaidam fault, view to east.

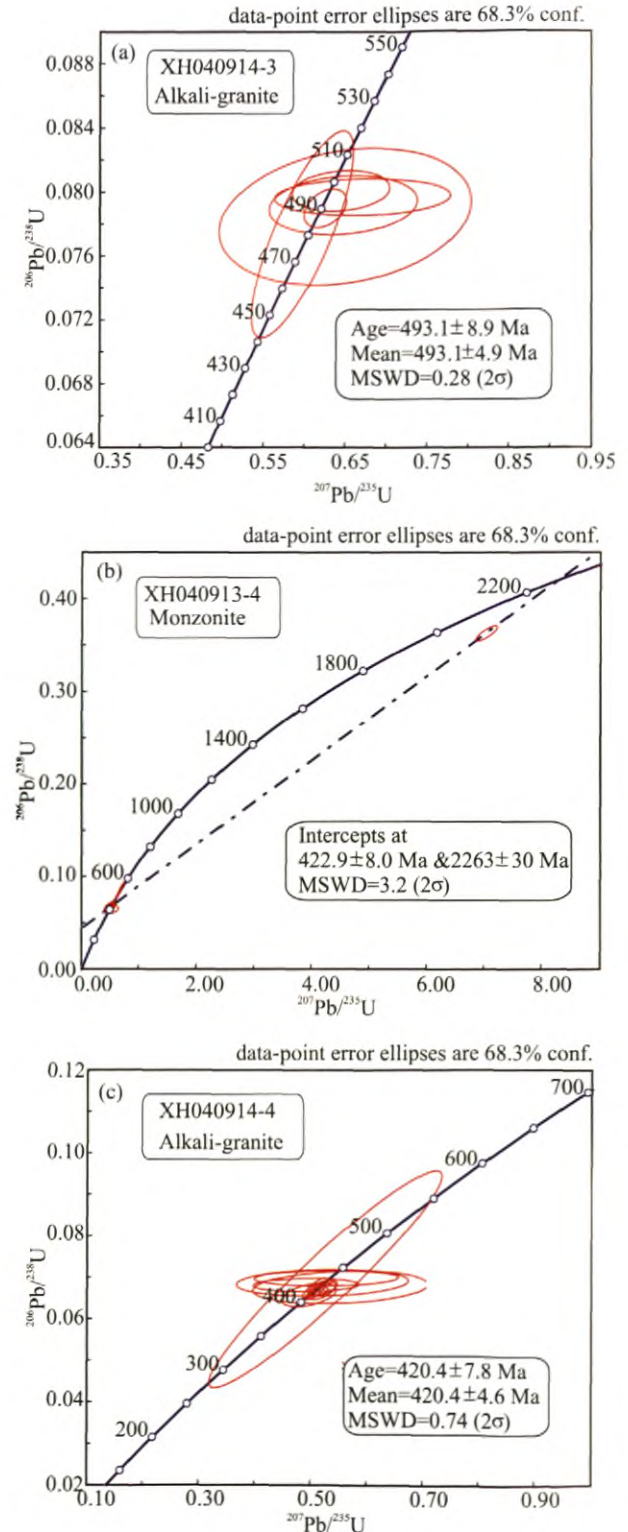


Fig. 5. Zircon $^{207}\text{Pb}/^{235}\text{U}$ – $^{206}\text{Pb}/^{238}\text{U}$ concordia diagrams of Early Paleozoic granitic samples from the basement of eastern Qaidam Basin.

represent the formation ages of granitic bodies through LA-ICP MS dating, this study tried to make two measurements for each zircon sample, one was at the core of the grain (marked by postfix C), the other at the rims (marked by postfix T). The ages obtained from the two tests were then compared (Fig. 7, in which the ages of single-grain zircons having inherited zircon cores were picked out). It can be deduced from the figure that the difference is not great between the ages of the zircon core (generally the upper limit) and that of the rim (generally the lower limit) of one zircon grain, so that they can represent the formation ages of granitic body.

3.2.1 Early Paleozoic magmatism

Sample XH040914-3 alkali-granite (location: 36°43.011'N, 98°51.280'E)

The sample is collected from east side of the intersection part of the north end of the Wenquan fault and the North Qaidam fault, which is dominated by right-lateral strike-slipping with steep dipping. It is brick red alkali-granite, consisting of quartz, K-feldspar and minor biotite. The granite body is deformed brittly with joints and locally developed quartz veins.

U, Th and Pb isotope analyses of 6 points from 4 zircon grains had been adopted for this sample after common Pb correction. All the 6 points are falling on the concordia line with almost concordant $^{206}\text{Pb}/^{238}\text{U}$ ages varying from 480 Ma to 497 Ma (Fig. 5a), yielding a weighted mean age of 493.1 ± 8.9 Ma (2σ), which may represent the crystallization and formation age of the alkali-granite in the Furongian Epoch of the Cambrian.

Sample XH040913-4 porphyroid monzonite (location: 37°00.242'N, 98°34.624'E)

Collected from the hanging wall near the North Qaidam fault north of Wulan Town, this sample is porphyroid monzonite with xenoliths of fine-grained diorite, composed mainly of plagioclase, K-feldspar and biotite, containing large plagioclase phenocrysts in 0.5 cm×1.5 cm. This is a small monzonite body, deformed ductily with flow structure and also brittly with joints, intruding into a fine-grained diorite body.

U, Th and Pb isotope analyses of 41 points from 24 zircon grains had been adopted for this sample after common Pb correction. Among them, the points 16T and 13C with slightly old ages and point 11C with an extra old age, are considered as odd outliers. Meanwhile, the other 38 points yield almost concordant ages with their apparent ages of $^{206}\text{Pb}/^{238}\text{U}$ ranging from 401 Ma to 452 Ma, showing the complicated magmatic history in the Early Paleozoic. The projected points fall on the concordia line or nearby in the concordia diagram (Fig. 5b), yielding a lower intercept age of 422.9 ± 8.0 Ma (2σ) and an upper

intercept age of 2263 ± 30 Ma (MSWD=3.2). The former is interpreted as the given crystallization age of the monzonite in the Ludlow Epoch of the Silurian, while the latter as the age of inherited zircons from the Qaidam Basin basement formed in the Hutuo Period of the Proterozoic.

Sample XH040914-4 alkali-granite (location: 36°42.623'N, 98°48.237'E)

It is collected from west-by-south side of the intersection part of the north end of the Wenquan fault and the North Qaidam fault. The sample is laterite-colored alkali-granite, consisting of quartz, K-feldspar and minor biotite, with joints and later quartz veins developed.

U, Th and Pb isotope analyses of 11 points from 11 zircon grains had been adopted for this sample after common Pb correction. All the 11 points yield very close ages with their apparent ages of $^{206}\text{Pb}/^{238}\text{U}$ varying from 410 Ma to 435 Ma. The projected points fall very well on the concordia line (Fig. 5c), yielding a weighted mean age of 420.4 ± 7.8 Ma (2σ), which may represent the crystallization and formation age of the alkali-granite in Ludlow Epoch of the Silurian.

3.2.2 Late Paleozoic-Early Mesozoic magmatism

Sample XH040913-3 K-feldspar granite (location: 37°16.676'N, 98°23.400'E)

The sample is medium- to coarse-grained K-feldspar granite, containing quartz, K-feldspar, plagioclase etc. It is collected from the undeformed granite body north of the hanging wall of the North Qaidam fault, some 18 km away from NQF.

U, Th and Pb isotope analyses of 28 points from 18 zircon grains had been adopted for this sample after common Pb correction. Among them, the points 4C and 3C yield some much older age data, being outliers; the other 26 points yield concordant ages, and the apparent ages of $^{206}\text{Pb}/^{238}\text{U}$ range from 244 Ma to 289 Ma. The projected points fall on the concordia line or nearby (Fig. 6a), yielding a weighted mean age of 257.8 ± 5.5 Ma (2σ), which may represent the crystallization and formation age of the K-feldspar granite in Lopingian Epoch of the Permian. The U-Pb age of point 3C, 444 ± 7.4 Ma, represents the age of the inherited zircon (with a rim age of 262.0 ± 16.4 Ma) formed in the Early Paleozoic (Late Ordovician) magmatism.

Sample XH040915-1 granodiorite (location: 36°24.149'N, 98°32.651'E)

It is collected from the location in-between the Elashan fault (ELSF) and the Dulan thrust (DT), being medium- to coarse-grained gray granodiorite, containing plagioclase, quartz, amphibole, K-feldspar, biotite etc., with a granitic texture. Joints are developed in the granodiorite body.

U, Th and Pb isotope analyses of 36 points from 20 zircon grains had been adopted for this sample after common Pb correction. Three points among them, i.e. 2C, 11T and 11C yield slightly old ages, being outliers. The other 33 points give concordant ages, and the apparent ages of $^{206}\text{Pb}/^{238}\text{U}$ range from 238 Ma to 289 Ma. The projected points fall on the concordia line in the concordia diagram (Fig. 6b), yielding a weighted mean age of 253.1 ± 5.4 Ma (2σ), which may represent the crystallization and formation age of the granodiorite in Lopingian Epoch of the Permian.

Sample XH040916-9 granodiorite (location: $35^{\circ}43.613'\text{N}$, $98^{\circ}06.863'\text{E}$)

Collected from the Yuegelu body on the hanging wall of the Boluoer fault, this sample is medium- to coarse-grained gray granodiorite, consisting of plagioclase, K-feldspar, quartz, biotite, amphibole etc., with schistosity developed. The rock body contains elongated fish-shaped melanocratic microgranular enclaves (MMEs), which are medium- to fine-grained porphyritic diorites containing plagioclase phenocrysts (Fig. 4b), with a length-width ratio of $\sim 5:1$, in en-echelon arrangement. The undeformed granodiorite near the outcrop of this sample is with a hypidiomorphic texture and massive structure, in which the plagioclase of andesine with $\text{An} = 47$ (Liu et al., 2004).

U, Th and Pb isotope analyses of 40 points from 20 zircon grains had been adopted for this sample after common Pb correction. With the exception of point 15C that yields an anomalously old age, being an outlier, all the other 39 points give concordant ages, and the apparent ages of $^{206}\text{Pb}/^{238}\text{U}$ range from 240 Ma to 300 Ma. The projected points fall on the concordia line in the concordia diagram (Fig. 6c), yielding a weighted mean age of 253.0 ± 4.6 Ma (2σ), which may represent the crystallization and formation age of the granodiorite in Lopingian Epoch of the Permian. Point 15C yields U-Pb age of 769.3 ± 23.9 Ma, while point 15T at the rim of the same grain gives an age of 261.5 ± 2.6 Ma. The age value of the granodiorite body yielded in the present study is slightly older than the SHRIMP II U-Pb age (242 ± 6 Ma) obtained by Liu et al. (2004) from the vicinity of this sample.

Sample XH040916-6 granodiorite (location: $35^{\circ}50.087'\text{N}$, $98^{\circ}09.347'\text{E}$)

It is collected from the north hanging wall of the South Qaidam fault, being granodiorite with MMEs in the body. U, Th and Pb isotope analyses of 38 points from 20 zircon grains had been adopted for this sample after common Pb correction. With exception of point 12C that yields a slightly old age, being an outlier, all the 37 points give concordant ages, and the apparent ages of $^{206}\text{Pb}/^{238}\text{U}$ vary

from 231 Ma to 306 Ma. The projected points fall on the concordia line in the concordia diagram (Fig. 6d), yielding a weighted mean age of 250.9 ± 5.1 Ma (2σ), which represents the crystallization and formation age of the granodiorite in the Early Triassic. Point 12C yields an age of 405.8 ± 17.5 Ma, which represents the crystallization age of inherited zircon formed in the Early Devonian of the Paleozoic, while the U-Pb age of point 12T at the rim of the same grain is 258.5 ± 3.6 Ma.

Sample XH040915-4 granodiorite (location: $36^{\circ}13.249'\text{N}$, $98^{\circ}25.816'\text{E}$)

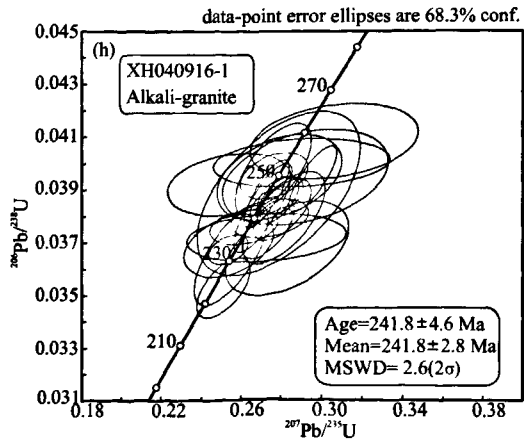
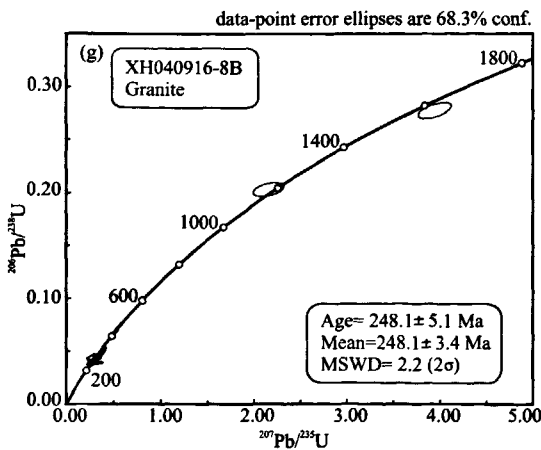
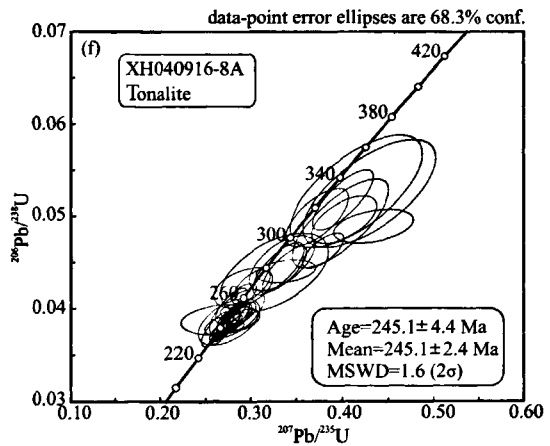
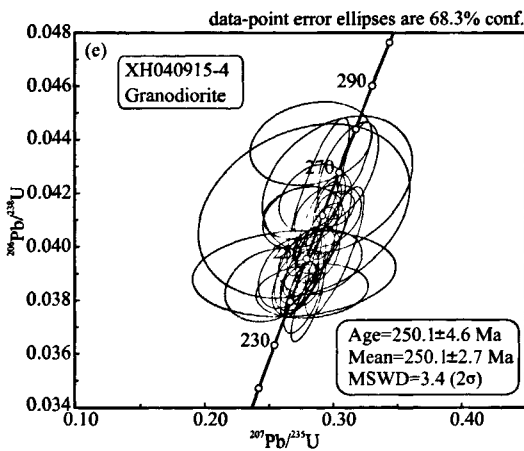
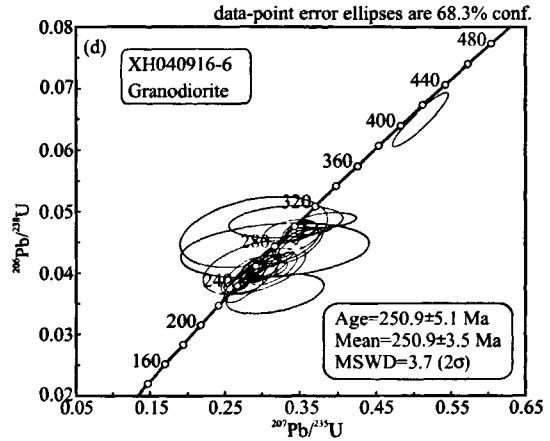
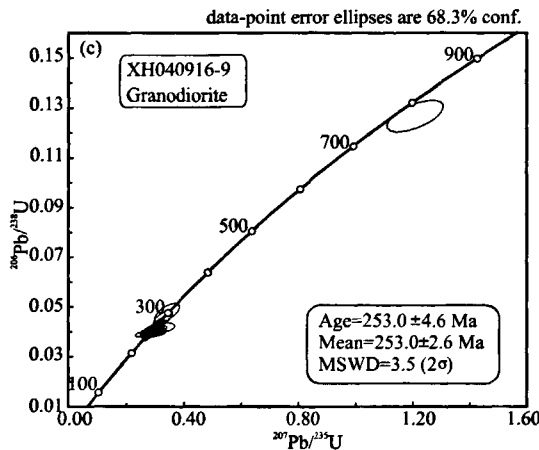
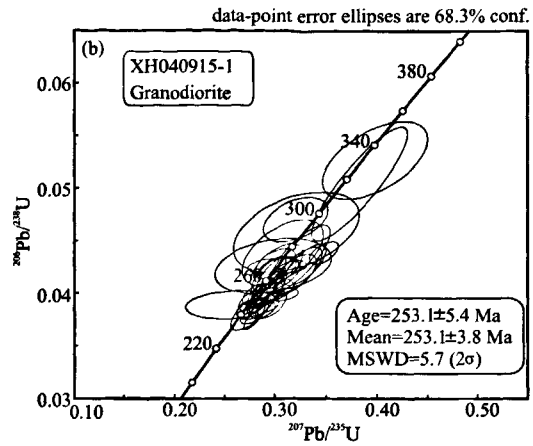
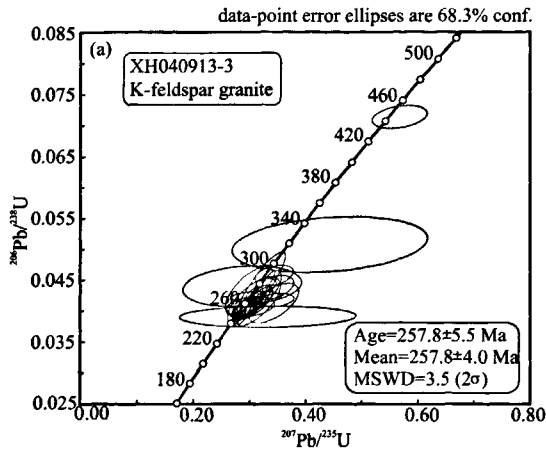
Collected from the southwest side of Yingteer Yangchang valley in the foot wall of the Hacipu fault, it is medium- to fine-grained granodiorite with no ductile deformation. U, Th and Pb isotope analyses of 35 points from 20 zircon grains had been adopted for this sample after common Pb correction. All the 35 points give very close ages, and the apparent ages of $^{206}\text{Pb}/^{238}\text{U}$ vary from 239 Ma to 279 Ma. The projected points fall on or near the concordia line in the concordia diagram (Fig. 6e), yielding a weighted mean age of 250.1 ± 4.6 Ma (2σ), which represents the crystallization and formation age of the granodiorite in the Early Triassic.

Samples XH040916-8A tonalite and XH040916-8B granite (location: $35^{\circ}45.375'\text{N}$, $98^{\circ}07.872'\text{E}$)

These two samples are collected from the hanging wall of the South Qaidam fault, close to the fault. The sample XH040916-8A is a tonalite, showing somewhat oriented arrangement of the minerals with weak schistosity, while the sample XH040916-8B is from a K-feldspar-rich red granite vein in the vicinity of the fault zone, consisting of K-feldspar and quartz, etc. The tonalite body contains a large amount of melanocratic microgranular enclaves (MMEs), generally in ellipsoidal or subangular forms with oriented long axes (Fig. 2a). Also developed in the tonalite body are numerous subparallel fine granular zones, 0.5-1 m thick, which may be attributed to deep-layered thrust faulting. Viewed from distance, the tonalite has layered features (Fig. 4).

U, Th and Pb isotope analyses of 39 points from 20 zircon grains had been adopted for the sample XH040916-8A after common Pb correction. Among them, 8 points, i.e., points 13C, 13T, 14C, 14T, 15C, 15T, 16C and 16T yield slightly old ages, being outliers. The other 31 points give concordant ages, and the apparent ages of $^{206}\text{Pb}/^{238}\text{U}$ vary from 234 Ma to 283 Ma. The projected points fall on the concordia line in the concordia diagram (Fig. 6f), yielding a weighted mean age of 245.1 ± 4.4 Ma (2σ), which represents the crystallization and formation age of the tonalite in the Early Triassic.

As for sample XH040916-8B, U, Th and Pb isotope analyses of 27 points from 18 zircon grains had been



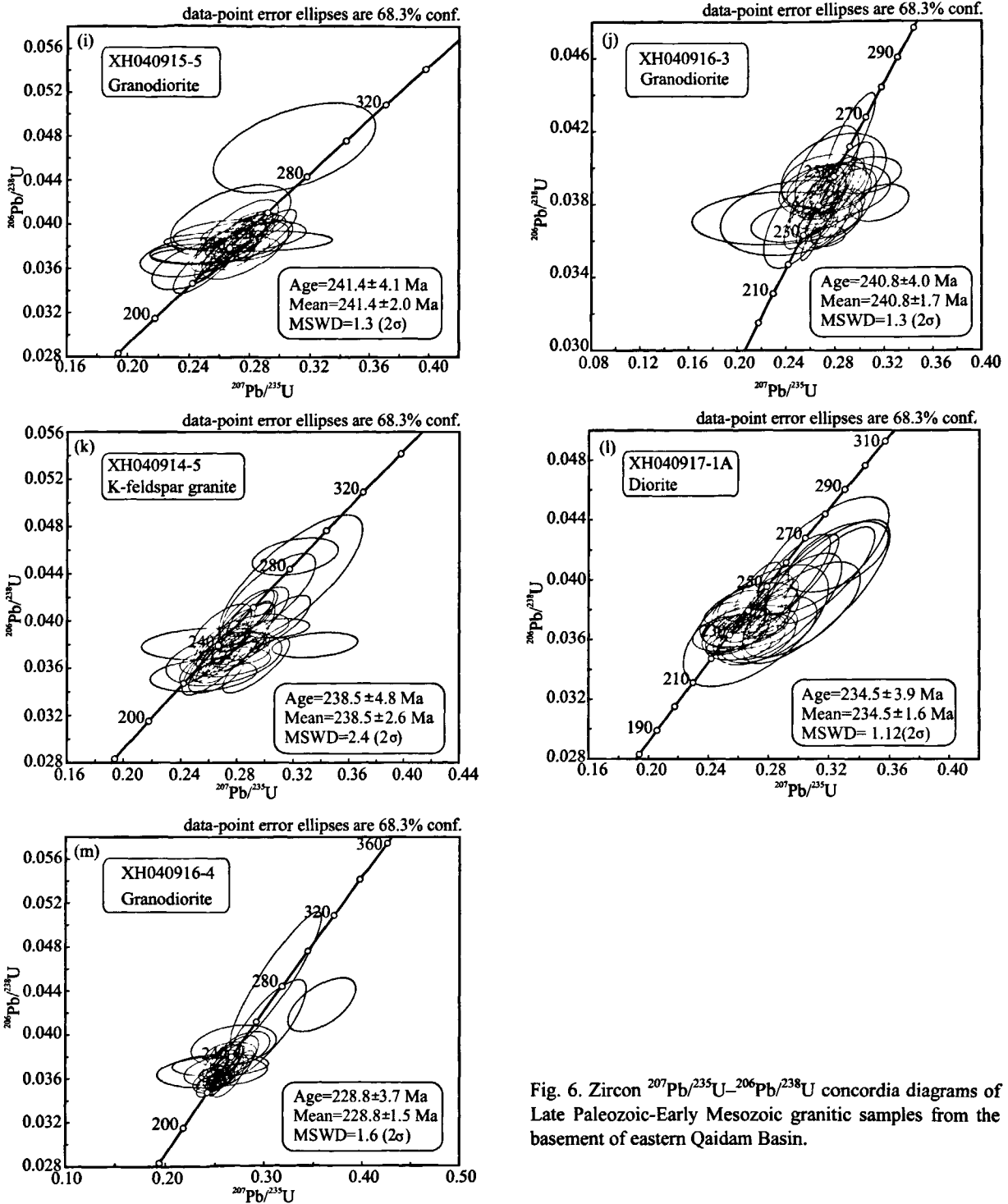


Fig. 6. Zircon $^{207}\text{Pb}/^{235}\text{U}$ - $^{206}\text{Pb}/^{238}\text{U}$ concordia diagrams of Late Paleozoic-Early Mesozoic granitic samples from the basement of eastern Qaidam Basin.

adopted after common Pb correction. Among them, points 6C, 12C, 19C and 4T yield slightly old ages, and points 10C and 16C yield anomalously old ages, being outliers. The other 21 points give concordant ages, and the apparent ages of $^{206}\text{Pb}/^{238}\text{U}$ vary from 235 Ma to 274 Ma. The projected points fall on the concordia line in the concordia diagram (Fig. 6g), yielding a weighted mean age of 248.1 ± 5.1 Ma (2σ), which represents the crystallization

and formation age of K-feldspar-rich granite in the Early Triassic. Point 16C of the sample yields an age of 1123.7 ± 90.5 Ma which may represents the formation age of the Mesoproterozoic basement in the Jixianian, while point 10C, with a rim age of 265.9 ± 11.2 Ma, yields an age of 1680.6 ± 44.5 Ma which may represents the formation age of the Mesoproterozoic basement in the early Changchengian.

Sample XH040916-1 alkali-granite (location: 36° 12.605'N, 98°09.957'E)

The sample is medium- to fine-grained red alkali-granite with joints, containing K-feldspar, quartz, etc. U, Th and Pb isotope analyses of 25 points from 20 zircon grains had been adopted after common Pb correction. All the 25 points give very close ages, and the apparent ages of $^{206}\text{Pb}/^{238}\text{U}$ vary from 223 Ma to 258 Ma. The projected points fall on or near the concordia line in the concordia diagram (Fig. 6h), yielding a weighted mean age of 241.8 ± 4.6 Ma (2σ), which represents the crystallization and formation age of the alkali-granite in the Middle Triassic.

Sample XH040915-5 granodiorite (location: 36° 15.314'N, 98°26.924'E)

Collected from the hanging wall of the Hacipu fault, close to the fault, the sample is porphyritic granodiorite with joints, containing K-feldspar phenocrysts in the size of 1.2 cm \times 2.5cm. U, Th and Pb isotope analyses of 38 points from 20 zircon grains had been adopted after common Pb correction. Among them, point 8C yields a slightly old age, being an outlier. The other 37 points give concordant ages, and the apparent ages of $^{206}\text{Pb}/^{238}\text{U}$ range from 229 Ma to 256 Ma. The projected points fall on the concordia line in the concordia diagram (Fig. 6i), yielding a weighted mean age of 241.4 ± 4.1 Ma (2σ), which represents the crystallization and formation age of the granodiorite in the Middle Triassic.

Sample XH040916-3 granodiorite (location: 36° 03.462'N, 98°07.045'E)

Collected from the middle segment of the Dulan-Xiangride highway, this sample is medium-grained red granodiorite, consisting of K-feldspar, plagioclase, quartz, biotite etc. The granodiorite body shows locally a porphyroid texture with K-feldspar phenocrysts, bedded joints and schistose textures. It contains some uneven distributed MMEs with diversified shapes, varied sizes and different compositions, dominated by dioritic matter. Some of them are round-shaped with size of ~ 7 cm. They are characterized by intensive flow plastic deformation. The boundaries between most enclaves and the host rocks are clear-cut, only a few are transitional, and cooling rims can sometimes be seen.

U, Th and Pb isotope analyses of 39 points from 20 zircon grains had been adopted for this granodiorite after common Pb correction. All the 39 points give very close ages, and the apparent ages of $^{206}\text{Pb}/^{238}\text{U}$ range from 227 Ma to 263 Ma. The projected points fall on or close to the concordia line in the concordia diagram (Fig. 6j), yielding a weighted mean age of 240.8 ± 4.0 Ma (2σ), which represents the crystallization and formation age of the granodiorite in the Middle Triassic.

Sample XH040914-5 K-feldspar granite (location: 36°33.630'N, 98°40.999'E)

It is undeformed medium- to fine-grained gray K-feldspar granite, collected from the central part of the gneiss rock body of the Proterozoic Shaliuhe Group far away from the various surrounding faults, containing K-feldspar, plagioclase, quartz, and biotite. The rock body shows slight variation in composition, being mostly K-feldspar granite and locally granodioritic.

U, Th and Pb isotope analyses of 42 points from 22 zircon grains had been adopted for this K-feldspar granite after common Pb correction. Among them, points 10C, 11C and 16C yield slightly old ages, being outliers. The other 39 points give concordant ages, and the apparent ages of $^{206}\text{Pb}/^{238}\text{U}$ range from 224 Ma to 260 Ma. The projected points fall on the concordia line in the concordia diagram (Fig. 6k), yielding a weighted mean age of 238.5 ± 4.8 Ma (2σ), which represents the crystallization and formation age of the K-feldspar granite in the Middle Triassic.

Sample XH040917-1A diorite (location: 36°06.443'N, 97°01.311'E)

It is gray diorite collected from a location of the old East Kunlun batholith on the way from Xiangride town to Golmud city. Fracturing, joints, and red granite veins ~ 1 m thick are developed in the diorite body. Some rock islands composed of diorites and granodiorites are developed on the south margin of the Qaidam Basin near this location, resulting in very irregular boundary between the southern Qaidam Basin and the Kunlun Mountains, which means that up-to-north thrusting is not developed very well in the area (Yin et al., 2007).

U, Th and Pb isotope analyses of 39 points from 20 zircon grains had been adopted for this diorite after common Pb correction. All the points yield very close concordant ages, and the apparent ages of $^{206}\text{Pb}/^{238}\text{U}$ range from 225 Ma to 263 Ma. The projected points fall on or near the concordia line in the concordia diagram (Fig. 6l), yielding a weighted mean age of 234.5 ± 3.9 Ma (2σ), which represents the crystallization and formation age of the diorite in the Middle Triassic.

Sample XH040916-4 granodiorite (location: 35° 57.575'N, 97°53.976'E)

It is medium-grained granodiorite collected also from the middle segment of the Dulan-Xiangride highway, consisting of K-feldspar, plagioclase, quartz, biotite etc, with porphyroid and linear flow structures. K-feldspar phenocrysts and MMEs are developed well in the granodiorite body.

U, Th and Pb isotope analyses of 39 points from 20 zircon grains had been adopted for this granodiorite after common Pb correction. Except that point 10C yields a

slightly old age, being an outlier, all the other 38 points give concordant ages, and the apparent ages of $^{206}\text{Pb}/^{238}\text{U}$ range from 222 Ma to 270 Ma. The projected points fall on the concordia line in the concordia diagram (Fig. 6m), yielding a weighted mean age of 228.8 ± 3.7 Ma (2σ), which represents the crystallization and formation age of the granodiorite in the Middle Triassic.

4 Discussions

4.1 Division of granitic magmatism stages of the eastern Qaidam Basin basement

At least 7 stages of Phanerozoic granitic magmatism, such as (1) >460 Ma, (2) 445–440 Ma, (3) 430–420 Ma, (4) 410–395 Ma, (5) 385–370 Ma, (6) 275–260 Ma, (7) 235–220 Ma, had been revealed by previous studies for the whole basement of Qaidam Basin and its surrounding orogenies (Harris et al., 1988; Bian et al., 2000, 2004; Wu et al., 2001, 2002, 2004a, b; Chen et al., 2002; Cowgill et al., 2003; Gehrels et al., 2003a; Chen et al., 2003a, b, 2004; Deng et al., 2004; Liu et al., 2004; Su et al., 2004; TIGMR, 2004; Meng et al., 2005; Wu et al., 2005; Zhang et al., 2005; Liu et al., 2006; Long et al., 2006; Chen et al., 2006; Menold, 2006; Mo et al., 2007; Wu et al., 2007; Lu et al., 2007; Guo et al., 2009; Menold et al., 2009; Chen et al., 2011a). Based on the statistics of LA-ICP MS zircon U-Pb ages of 523 points from 297 zircon grains of 16 granitoid samples from the basement of the eastern Qaidam Basin, an age spectral diagram of the basement magmatism of the eastern Qaidam Basin is obtained (Fig. 8), suggesting that there are 3 peak ages of the tectono-magmatism (Fig. 8) in the basement of the eastern Qaidam Basin in the Phanerozoic. Among them, the main stage, which may be called as Stage III in the time sequence, has the peak age of magmatism at 244 Ma with weighted mean ages range from 257.8 ± 4.0 to 228.8 ± 1.5 Ma (13 samples), deviating a little bitter from the stage division above. The second stage, which may be called as Stage II, has the peak age of magmatism at 418 Ma with weighted mean ages range from 422.9 ± 8.0 to 420.4 ± 4.6 Ma (2 samples), corresponding to the stage 3 mentioned above. The minor stage, which may be called as Stage I in the time sequence, has a peak age of 493 Ma (1 sample) with a weighted mean age of 493.1 ± 4.9 Ma, corresponding to the stage 1.

There is only one sample for the Stage I magmatism in the Late Cambrian–Early Ordovician, which is the sample XH040914-3 with zircon U-Pb age of 493.1 ± 4.9 Ma (2σ), collected from the northeast side of the Wenquan fault. It reflects the beginning of Phanerozoic basement magmatism of the eastern Qaidam Basin (and even other areas surrounding the basin), which is consistent with the

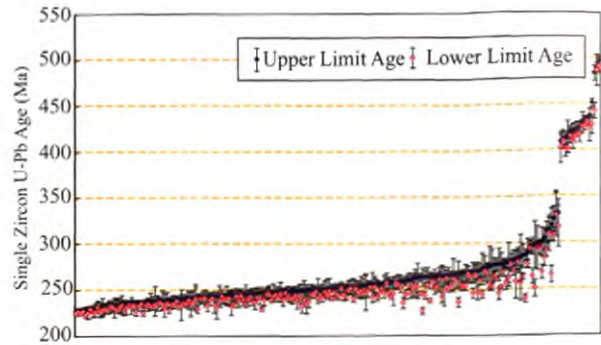


Fig. 7. Comparison of Zircon $^{207}\text{Pb}/^{235}\text{U}$ – $^{206}\text{Pb}/^{238}\text{U}$ concordant ages of the cores and rims of crystals from plutons in the eastern Qaidam Basin basement. All the significantly older (inherited) “core” ages are excluded.

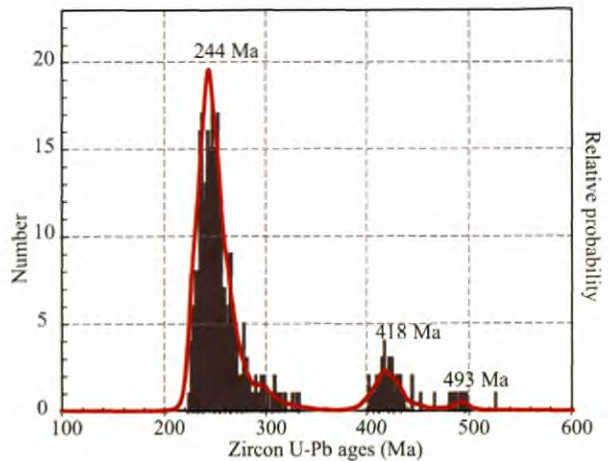


Fig. 8. Zircon $^{207}\text{Pb}/^{235}\text{U}$ – $^{206}\text{Pb}/^{238}\text{U}$ age distribution of the adopted 523 points analyzed in this study for the magmatism since the Early Paleozoic in the eastern Qaidam Basin basement.

beginning of the formation of north Qaidam ultra-high pressure metamorphic zone at 495 Ma (Xu et al., 2003; Mattinson et al., 2007).

The Stage II magmatism may lie in the range of 450 Ma to 400 Ma with a peak age of 418 Ma (Fig. 8), which is mainly reflected by and younger than the 2 samples with weighted mean ages of 422.9 ± 8.0 Ma and 420.4 ± 4.6 Ma, respectively. They are occurring from the north side of the Dulan thrust to both sides of the North Qaidam fault. Also, the stage II magmatism is reflected by some inherited zircon grains (generally cores) captured during the Stage III magmatism. Stage II peak magmatism is consistent with the end of HP/UHP metamorphism in the eastern North Qaidam between 459 Ma to 422 Ma (Mattinson et al., 2007), but slightly earlier than the final exhumation of the UP/UHP rocks in the north Qaidam ultra-high pressure metamorphic zone during 400–406 Ma (Xu et al., 2003).

SHRIMP zircon U-Pb age of 397 ± 3 Ma reported by Wu C. et al. (2004a) from granodiorite in the North Yematan granite body near Dulan town could be the youngest age of stage II magmatism.

A total of 13 samples (I-type granitoids; Chen et al., 2011a) from the analyzed 16 granitoid samples have their weighted mean ages ranging from 257.8 Ma to 228.8 Ma, being of the P-T, which reflects the stage III magmatism with a peak age of 244 Ma (Fig. 8). Among them, the sample XH040913-3 with the oldest age at 257.8 Ma (Late Permian) occurs in the South Qilian magmatic belt dominated by Stage-II magmatism in the Early Paleozoic on the north side of the North Qaidam fault. It may represent the northmost location and beginning point of the Late Permian-Middle Triassic (P-T) magmatism during stage III magmatism (Figs. 1 and 9). The youngest age (228.8 Ma) of stage III magmatism appears at a central position of the P-T magmatism of granodiorite in the vicinity of Xiangride town (Figs. 1 and 9).

According to the above analysis, the present study makes a modification of the division of magmatic zones on the southeast margin of the Qaidam Basin. For example, Sun et al. (2001) considered that there are two magmatic arcs in the eastern Qaidam Basin basement, one is the Late Paleozoic East Kunlun magmatism belt at the south margin of the Qaidam Basin, and another one is the Elashan magmatism belt on the east margin of the Qaidam Basin in the Late Triassic. Tianjin Institute of Geology and Mineral Resources (2004) divided the eastern Qaidam Basin basement magmatic zone into the early-stage East Kunlun Xiangride sequence (Late Permian-Middle Triassic) and the late-stage Elashan Kekesai intrusive sequence (Mid-Late Triassic). However, the age data given in this study show that, except the Early Paleozoic magmatism, all the ages of magmatic intrusion from the East Kunlun Mountains to the South Qilian Mountains in the eastern Qaidam Basin basement are concentrated in the Late Permian to Middle Triassic, and that magmatism was relatively weak in the Late Triassic. Therefore, a series of NW- to WNW-extending mountain chains cut by the Eastern Qaidam thrust system, e.g. the Wahong, Ela, Hacipu, Senmucike, South Xiangjia and Buerhanbuda (of the East Kunlun) mountains, actually belong to a unified and inseparable Permian-Triassic magmatic system.

4.2 Relationship between magmatisms in eastern Qaidam Basin basement and its surrounding areas

On the basis of LA-ICP MS zircon U-Pb dating of magmatism in eastern Qaidam Basin basement, and in combination with the results from previous researches, it is considered that the Early Paleozoic granitoid magmatism occurred mainly on the north margin of the

Qaidam and south margin of the Qilian Mountains, with only weak indications in the East Kunlun Mountains. However, the distribution of P-T granitoids runs through the whole Qaidam Basin basement from the East Kunlun northward to the south margin of the Qilian Mountains (Figs. 1 and 9). Therefore, the P-T granitoids are the main component of the basement of the eastern Qaidam Basin.

Taking a comprehensive view of the Qaidam Basin and its surrounding areas (Fig. 9), the granitoid magmatisms from the Early Paleozoic to early Late Paleozoic (493-379 Ma) are mainly distributed in the Altyn Tagh Mountains (Gehrels et al., 2003a; Chen X. et al., 2003a,b, 2004), the Qilian Mountains -north margin of Qaidam (Wu C. et al., 2001, 2004a; Cowgill et al., 2003; Gehrels et al., 2003a, b; Su et al., 2004; Meng et al., 2005) and the Qimantag area (Chen H. et al., 2006), and there are also a few distributions in the East Kunlun Mountains (Zhang et al., 2005; Long et al., 2006). The peak ages of granitoid intrusion in the Altyn Tagh and south Qilian mountains are 443 Ma (Chen X. et al., 2003b) and 446-440 Ma (Lu et al., 2007; Menold et al., 2006; Gehrels et al., 2003a; Wu C. et al., 2002) respectively, which correspond to the North Qaidam HP/UHP metamorphism between 459 Ma to 422 Ma (Mattinson et al., 2007). Retrograde metamorphic eclogite xenoliths often occur on the rims of some intrusive plutons in this stage. In addition, from the North Qilian via northern Qaidam to the Qimantag and East Kunlun mountains, the magmatisms of granitoids in this time duration show a general trend of going younger gradually from North to South.

Nevertheless, the existing Qaidam Basin basement is obviously penetrated by P-T granitoid magmatisms. The earliest P-T plutons of leucogranites and quartz diorites with U-Pb ages range from 293.6 Ma to 270 Ma were exposed along the north central margin of the Qaidam basin at Damenkou area (Gehrels et al., 2003a; Fig. 9), marking the start of P-T granitoid magmatisms in the Qaidam Basin basement. Besides, there are granites of 260 Ma in Yuka pluton (Menold et al., 2006) and of 242.6 ± 3.2 Ma in Lenghu pluton (Yang and Song, 2002) in northern Qaidam, granites of 246 Ma, 238 Ma, and 215 Ma respectively from Tianjun Nan Shan, Qinghaihu Nan Shan, and Erlangdong plutons in Zongwulong belt (Guo et al., 2009), MMEs of 242 ± 6 Ma in granodiorite with an age of 241 ± 5 Ma and bojite of 239 ± 6 Ma from Yuegelu body in eastern segment of the East Kunlun (Liu et al., 2004), and granitoids of 241-236 Ma in middle segment of the East Kunlun Mountains (Harris et al., 1988; Zhang et al., 2005). The U-Pb ages listed above and provided by this study reflect the extending of magmatisms from west to east and from north to south (Fig. 9). U-Pb ages of P-T granitoids are also available in the Qimantag Mountains,

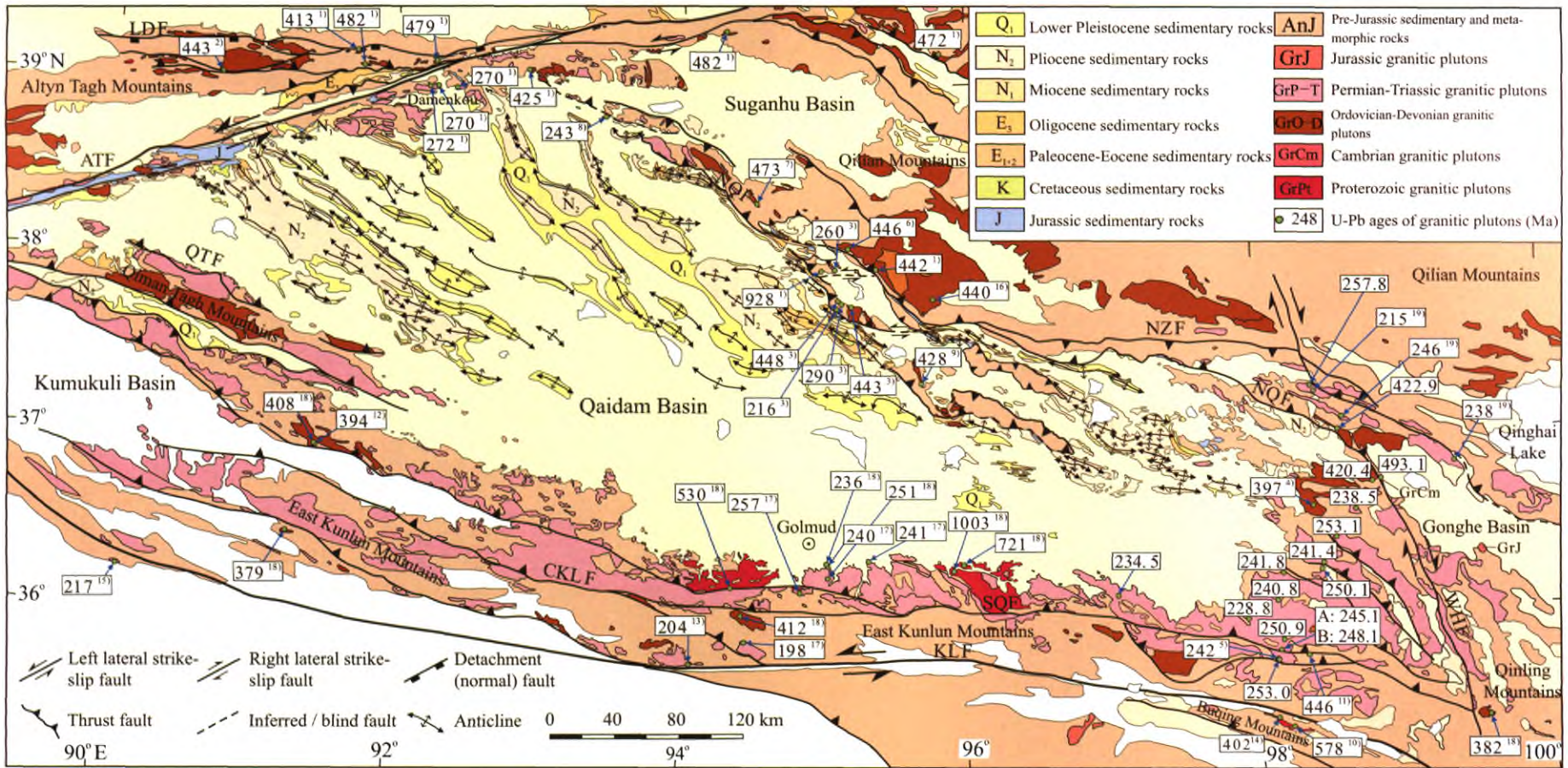


Fig. 9. Zircon U-Pb age distribution showing Paleozoic and Mesozoic magmatism in the Qaidam Basin basement. Explanation: NZF, north Zongwulongshan fault. NQF, north Qaidam fault. QTF, north Qimantag fault. SQF, south Qaidam fault. KLF, Kunlun fault. ATF, Altyn Tagh fault. WHF, Wahongshan fault (Wenquan fault). LDF, Lapeiquan detachment fault (Chen X. et al., 2003a). Age data are from: 1) Gehrels et al., 2003a; 2) Chen X. et al., 2004; 3) Menold, 2006; 4) Wu C. et al., 2004b; 5) Liu C. et al., 2004; 6) Wu C. et al., 2001a; 7) Wu C. et al., 2001b; 8) Yang and Song, 2002; 9) Meng et al., 2005; 10) Bian et al., 2000; 11) Wang et al., 2003; 12) Chen H. et al., 2006; 13) Wu Z. et al., 2005; 14) Bian et al., 2004; 15) Roger et al., 2003; 16) Lu et al., 2007; 17) Harris et al., 1988; 18) Zhang et al., 2005; 19) Guo et al., 2009, and this study.

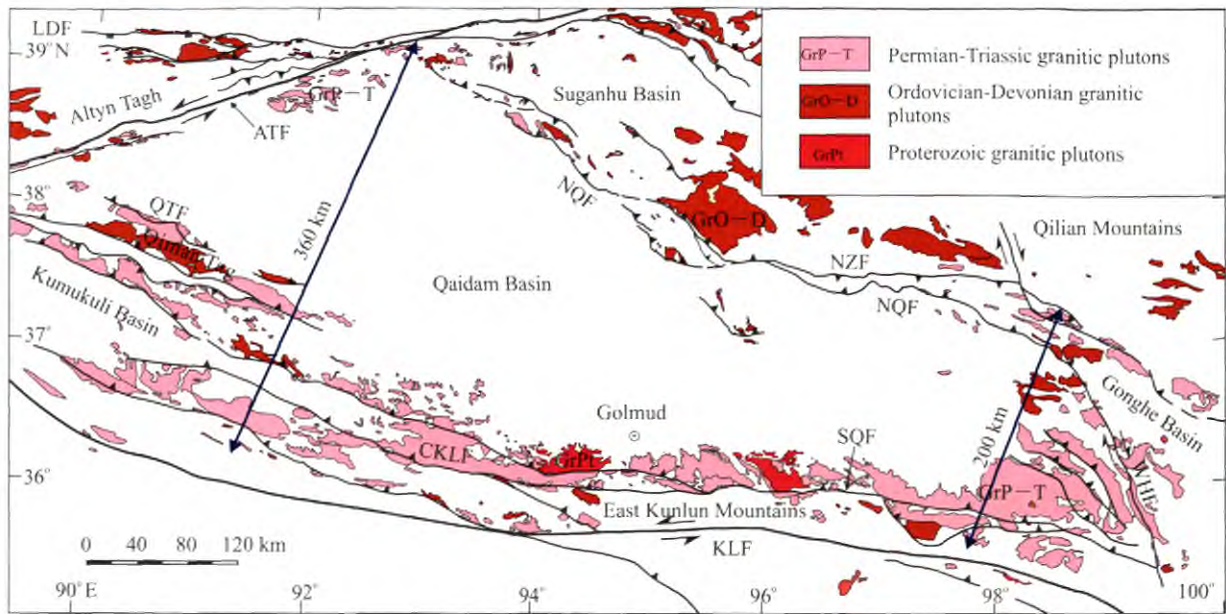


Fig. 10. Simplified map showing the change of widths of the P-T magmatic zone from western (~360 km) to eastern (~200 km) parts of the Qaidam Basin basement.

the northwestern segment of the East Kunlun Mountains (Jiang et al., 1992; QBGM, 1991; Chen D. et al., 2001). In particular, the P-T magmatism with U-Pb ages of 257.8–228.8 Ma in the eastern Qaidam Basin basement provided by this study directly suggest the widespread of basement magmatism in this period, and provide a chronological supporting for the anti-Bowen's reaction series (Chen et al., 2011a) and the underplating of mafic magma from the mantle and dynamic mixing between the mantle-derived mafic and crust-derived felsic magmas (Deng et al., 2004; Mo et al., 2007).

The latest P-T magmatism with ages in the Late Triassic occur scatteredly as small plutons on the northern margin of the Qaidam Basin and southern part of the East Kunlun Mountains, respectively (Fig. 9). For example, there are Da Qaidam granite of 216 ± 2.0 Ma in the northern Qaidam (Menold et al., 2009), Xidatan granite of 205 ± 13 Ma (Chen W. et al., 2002) and 204.1 ± 2.6 Ma (Wu Z. et al., 2005) and Xidatan granitic gneiss of 194 ± 17 Ma (Pan et al., 1998) in the East Kunlun Mountains, and Jingren syenogranite of 204.1 ± 2.6 Ma in the Yemaquan area, Qimantag Mountains (Liu et al., 2006). That suggests the magmatism might have lasted into the Early Jurassic.

Therefore, just as Yin and Harrison (2000) pointed out, the P-T plutons in the South Qilian and north Qaidam Basin are possibly the extending of the grand P-T batholith in the East Kunlun Mountains. That is to say, during the P-T period, the whole Qaidam Basin basement and its surrounding orogens had undergone extensive magmatic intrusions.

4.3 Shortening of the Qaidam Basin basement as viewed from the spatial distribution of Permian-Triassic magmatism

On the basis of age distribution of granitoid magmatism in the Qaidam Basin basement and its surrounding mountain systems (see Fig. 9), we can roughly draw the spatial outline of P-T magmatism, which is a strip-shaped zone bounded by the Altyn Tagh, North Qaidam / North Zongwulongshan and Kunlun faults. Eastward it may run across the Wenquan fault to join the West Qinling magmatic zone (Fig. 10). For example, many adakitic granites of 245–238 Ma along the Xiahe-Lixian area in the West Qinling Mountains (Jin et al., 2005), are consistent in age with the P-T magmatism in the eastern Qaidam Basin basement, indicating that the subduction and crustal thickening event occurring in the eastern Qaidam Basin basement is the same as in the northern Paleo-Tethys Ocean.

Regarding to the strip-shaped P-T magmatic zone in the Qaidam Basin basement and its surrounding orogens, its width (roughly N-S) is decreasing gradually from ~360 km (a little bit less than 400 km estimated by Gehrels et al., 2003) in the west to 200 km in the east (Fig. 10). Many explanations could be made for this. We prefer to that, if the original widths of this south facing arc system (Gehrels et al., 2003) are approximately the same from west to east, then the width of the magmatic zone in eastern Qaidam is estimated to be shortened by ~44% relative to that in western Qaidam, i.e., the shortening of

the basin basement tended to intensify from west to east, reaching its maximum in eastern Qaidam at ~44%.

According to the field observation and structural relationship analysis, the relative shortening of the basin basement is closely related to the thrust faulting developed in the basement, and the development of Cenozoic thrust faults is the main cause for the shortening of the basin basement. Cenozoic thrust faults developed well in the eastern Qaidam region, such as North Qaidam, Elashan, Hacipu, Chahanwusu, Gouli and South Qaidam faults of the Eastern Qaidam thrust system, resulted in the shortening of the eastern Qaidam basement and the less thickness of the Cenozoic sedimentation there (Jiang et al., 2008; Chen et al., 2011b). Meanwhile, the huge thickness of the Cenozoic sediments in western Qaidam, which is a reserve base of the Qaidam modern salt lake potash industry (Zheng et al., 2011), may reflect the poor developed thrusting and so that the less shortening of the western Qaidam basement.

The difference in basement deformation as reflected by the width variation of magmatic zones between the eastern and western Qaidam basement makes a striking contrast to the difference in the Cenozoic shortening of the sedimentary cover in the Qaidam basin. In western Qaidam, the shortening of Cenozoic sedimentary layers is over 48%, while in eastern Qaidam, Cenozoic sedimentary layers are poorly developed with shortening below 1% (Yin et al., 2008b). Thus, the crustal shortening in western Qaidam is over 40% relative to that in eastern Qaidam in terms of Cenozoic sedimentary layers. The difference in shortening between basement and sedimentary cover, as well as its variation along the basin's long axis nearly E-W, shows that there was a transformation of the crust shortening and thickening between the eastern and western Qaidam Basin. That is, crust shortening in eastern Qaidam was dominated by the deformation of basement representing the middle and lower crust, whereas it was by the deformation mainly of sedimentary cover representing the upper crust in western Qaidam.

5 Conclusions

On the basis of LA-ICP MS zircon U-Pb geochronology of the basement magmatisms in the eastern Qaidam Basin that lies at the intersection of the Qinling, Qilian and Kunlun orogens, and together with the geochronological results by previous researches, the following conclusions are arrived at in this paper.

(1) The eastern Qaidam Basin basement, from the northern margin of the Qaidam Basin to the East Kunlun Mountains, has mainly experienced three stage intrusive magmatisms of granitoids since the Early Paleozoic,

which are the magmatisms occurring in the Late Cambrian - Early Ordovician (stage I), the Silurian - Devonian (stage II), and the Late Permian - Middle Triassic (stage III), with the peak ages being 493 Ma, 418 Ma and 244 Ma, respectively. Among them, the granitoids of stage III form the main component of the basement of the eastern Qaidam Basin.

(2) The Early Paleozoic magmatism of granitoids mainly occurred in the northern margin of the Qaidam Basin and the Qilian Mountains, with only weak indications in the East Kunlun Mountains.

(3) The P-T magmatisms of granitoids occurred in the whole Qaidam Basin basement, from the south Qilian Mountains and the north margin of the Qaidam Basin, through the whole basin, to the East Kunlun Mountains. It began in the northwestern margin of the Qaidam Basin during 293.6-270 Ma, and expanded eastwards and southwards, resulting in P-T intrusive magmatism which run through the whole basin basement.

Acknowledgements

We would like to thank the Arizona LaserChron Center, University of Arizona for the help in LA-ICP MS zircon U-Pb dating. The reviewers made several suggestions helping improve the original manuscript. Financial supports by the Basic Research Foundation of the Institute of Geomechanics, CAGS, China (DZLXJK200703), the National Natural Science Foundation of China (40342015), SinoProbe - Deep Exploration in China (SinoProbe-08), and the National Science Foundation (USA) Instrumentation and Facilities Program (EAR-0443387) are gratefully acknowledged.

Manuscript received May 8, 2011

accepted Sept. 7, 2011

edited by Fei Hongcai

References

- Andersen, T., 2002. Correction of common lead in U-Pb analyses that do not report ^{204}Pb . *Chem. Geol.*, 192 (1/2): 59-79.
- Bian, Q.T., Li, D.H., Pospelov, I., Yin, L.M., Li, H.S., Zhao, D.S., Chang, C.F., Luo, X.Q., Gao, S.L., Astrakhansev, O., and Chamov, N., 2004. Age, geochemistry and tectonic setting of Buqingshan ophiolites, North Qinghai-Tibet Plateau, China. *Journal of Asian Earth Sciences*, 23: 577-596.
- Bian, Q., Luo, X., Li, D., Zhao, D., Chen, H., Xu, G., Chang, C., and Gao, Y., 2000. Discovery of Caledonian island-arc granodiorite-tonalite in Buqingshan, Qinghai Province. *Progress in Natural Science*, 10 (1): 74-78.
- Chen Danling, Liu Liang, Che Zicheng, Luo Jinhai and Zhang Yunxiang, 2001. Determination and preliminary study of Indosinian aluminous A-type granites in the Qimantag area,

- southeastern Xinjiang. *Geochimica*, 30 (6): 540–546 (in Chinese with English abstract).
- Chen Hongwei, Luo Zhaohua, Mo Xuanxue, Zhang Xueting, Wang Jin and Wang Bingzhang, 2006. SHRIMP ages of Kayakedengtage complex in the East Kunlun Mountains and their geological implications. *Acta Petrologica et Mineralogica*, 25 (1): 25–32 (in Chinese with English abstract).
- Chen Wen, Zhang Yan, Ji Qiang, Wang Songshan and Zhang Jianxin, 2002. Magmatism and deformation times of the Xidatan rock series, East Kunlun Mountains. *Science in China (Series B)*, 45 (Supp.): 20–27.
- Chen Xuanhua, Yin An, George Gehrels, Li Li and Jiang Rongbao, 2011a. Chemical geodynamics of granitic magmatism in the basement of the eastern Qaidam Basin, northern Qinghai-Tibet Plateau. *Acta Geologica Sinica*, 85 (2): 157–171 (in Chinese with English abstract).
- Chen Xuanhua, McRivette M.W., Li Li, Yin An, Jiang Rongbao, Wan Jinglin and Li Huijun, 2011b. Thermochronological evidence for multi-phase uplifting of the East Kunlun Mountains, northern Tibetan Plateau. *Geological Bulletin of China*, 30 (11): 1647–1660 (in Chinese with English abstract).
- Chen Xuanhua, Dang Yuqi, Yin An, Wang Liqun, Jiang Wuming, Jiang Rongbao, Zhou Suping, Liu Mingde, Ye Baoyin, Zhang Min, Ma Lixie and Li Li, 2010. *Basin-mountain coupling and tectonic evolution of Qaidam Basin and its adjacent orogenic belts*. Beijing: Geological Publishing House, 1–365 (in Chinese).
- Chen Xuanhua, Wang Xiaofeng, George Gehrels, Yang Yi, Qin Hong, Chen Zhengle, Yang Feng, Chen Bailin and Li Xuezhi, 2004. Early Paleozoic magmatism and gold mineralization in north Altyn Tagh, NW China. *Acta Geologica Sinica (English Edition)*, 78 (2): 515–523.
- Chen Xuanhua, Yin, A., Gehrels, G.E., Cowgill, E.S., Grove, M., Harrison, T.M., and Wang, X.F., 2003a. Two phases of Mesozoic north-south extension in the eastern Altyn Tagh range, northern Tibetan Plateau. *Tectonics*, 22(5): 1053, doi: 10.1029/2001TC001336.
- Chen Xuanhua, George Gehrels, Wang Xiaofeng, Yang Feng and Chen Zhengle, 2003b. Granite from North Altyn Tagh, NW China: U-Pb geochronology and tectonic setting. *Bulletin of Mineralogy, Petrology and Geochemistry*, 22 (4): 294–298 (in Chinese with English abstract).
- Chen Zhengle, Wang Xiaofeng, Yin An, Chen Bailin and Chen Xuanhua, 2004. Cenozoic left-slip motion along the central Altyn Tagh fault as inferred from the sedimentary record. *International Geology Review*, 46: 839–856.
- Chen Zhengle, Wan Jinglin, Wang Xiaofeng, Chen Xuanhua, Pan Jinhua, 2002. Rapid strike-slip of the Altyn Tagh Fault at 8 Ma and its geological implications. *Acta Geoscientia Sinica*, 23 (4): 295–300 (in Chinese with English abstract).
- Cowgill, E., Yin, A., Harrison, T.M., and Wang, X., 2003. Reconstruction of the Altyn Tagh fault based on U-Pb geochronology: Role of back thrusts, mantle sutures, and heterogeneous crustal strength in forming the Tibetan Plateau. *J. Geophys. Res.*, 108(B7): 2346, doi: 10.1029 / 2002 JB002080.
- Deng Jinfu, Luo Zhaohua, Su Shangguo, Mo Xuanxue, Yu Bingsong, Lai Xingyun and Chen Hongwei, 2004. *Petrogenesis, Tectonic Environment and Metallogenesis*. Beijing: Geological Publishing House, 1–381 (in Chinese).
- Gehrels, G.E., Valencia, V.A., and Ruiz, J., 2008. Enhanced precision, accuracy, efficiency, and spatial resolution of U-Pb ages by laser ablation-multicollector-inductively coupled plasma-mass spectrometry. *Geochem. Geophys. Geosyst.*, 9: Q03017, doi:10.1029/2007GC001805.
- Gehrels, G., Valencia, V., and Pullen, A., 2006. Detrital zircon geochronology by laser ablation multicollector ICP MS at the Arizona LaserChron Center. In: Olszewski, T.(ed.), *Geochronology: Emerging Opportunities*. Paleontology Society Papers, 12: 67–76.
- Gehrels, G.E., Yin, A., and Wang, X.F., 2003a. Magmatic history of the northeastern Tibetan Plateau. *J. Geophys. Res.*, 108 (B9), 2423, doi: 10.1029 / 2002 JB001876.
- Gehrels, G.E., Yin, A., and Wang, X.F., 2003b. Detrital-zircon geochronology of the northeastern Tibetan Plateau. *GSA Bulletin*, 115 (7): 881–896.
- Guo, A.L., Zhang, G.W., Qiang, J., Sun, Y.G., Li, G., and Yao, A.P., 2009. Indosinian Zongwulong orogenic belt on the northeastern margin of the Qinghai-Tibet plateau. *Acta Petrologica Sinica*, 25 (1): 1–12 (in Chinese with English abstract).
- Harris, N.B.W., Xu, R., Lewis, C.L., Hawkesworth, C.J., and Zhang, Y., 1988. Isotope geochemistry of the 1985 Tibet Geotraverse, Lhasa to Golmud. *Philos. Trans. R. Soc. London*, A327: 263–285.
- Johnston, S., Gehrels, G., Valencia, V., and Ruiz, J., 2009. Small-volume U-Pb zircon geochronology by laser ablation-multicollector- ICP-MS. *Chemical Geology*, 259: 218–229.
- Jiang Chunfa, Yang Jingsui, Feng Bingui, Zhu Zhizhi, Zhao Min and Chai Yaochu, 1992. *Opening-closing tectonics of the Kunlun Mountains*. Beijing: Geological Publishing House, 1–224 (in Chinese with English abstract).
- Jiang Rongbao, Chen Xuanhua, Dang Yuqi, Yin An, Wang Liqun, Jiang Wuming, Wan Jinglin, Li Li, and Wang Xiaofeng, 2008. Apatite fission track evidence for two phases Mesozoic-Cenozoic thrust faulting in eastern Qaidam Basin. *Chinese Journal of Geophysics*, 51 (1): 116–124 (in Chinese with English abstract).
- Jin Weijun, Zhang Qi, He Dengfa and Jia Xiuqin, 2005. SHRIMP dating of adakites in western Qinling and their implications. *Acta Petrologica Sinica*, 21 (3): 959–966 (in Chinese with English abstract).
- Liu Chengdong, Mo Xuanxue, Luo Zhaohua, Yu Xuehui, Chen Hongwei, Li Shuwei and Zhao Xin, 2004. Mixing events between the crust- and mantle-derived magmas in Eastern Kunlun: Evidence from zircon SHRIMP II chronology. *Chinese Science Bulletin*, 49 (8): 828–834.
- Liu Xun and Gao Rui, 1998. The crustal structure and assembly of terranes in the Qaidam-Qilian-Beishan Area, Western China. *Acta Geologica Sinica (English Edition)*, 72 (3): 243–255.
- Liu Yunhua, Mo Xuanxue, Yu Xuehui, Zhang Xueting and Xu Guowu, 2006. Zircon SHRIMP U-Pb dating of the Jingren granite, Yemaquan region of the east Kunlun and its geological significance. *Acta Petrologica Sinica*, 22 (10): 2457–2463 (in Chinese with English abstract).
- Long Xiaoping, Jin Wei, Ge Wenchun and Yu Neng, 2006. Zircon U-Pb geochronology and geological implications of the granitoids in Jinshuikou, East Kunlun, NW China. *Geochimica*, 35 (4): 333–345 (in Chinese with English abstract).

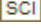
- Lu Xinxiang, Sun Yanggui, Zhang Xueting, Xiao Qinghui, Wang Xiaoxia, Wei Xiangdong and Gu Demin, 2007. The SHRIMP age of Tatalin rapakivi granite at the north margin of Qaidam Basin. *Acta Geologica Sinica*, 81 (5): 626–634 (in Chinese with English abstract).
- Ludwig, K.R., 2003. *Isoplot 3.00*. Berkeley Geochronology Center, Special Publication, 4: 1–70.
- Mattinson, C., Menold, C., Zhang, J., and Bird, D., 2007. High- and ultrahigh-pressure metamorphism in the North Qaidam and South Altyn terranes, western China. *International Geology Review*, 49: 969–995.
- Mattinson, C.G., Wooden, J.L., Liou, J.G., Bird, D.K., and Wu, C.L., 2006. Geochronology and tectonic significance of Middle Proterozoic granitic orthogneiss, North Qaidam HP/UHP terrane, Western China. *Mineralogy and Petrology*, 88: 227–241.
- Meng Fancong, Zhang Jianxin and Yang Jingsui, 2005. Tectono-thermal event of post-HP/UHP metamorphism in the Xitieshan area of the North Qaidam Mountains, western China: Isotopic and geochemical evidence of granite and gneiss. *Acta Petrologica Sinica*, 21 (1): 45–56 (in Chinese with English abstract).
- Menold, C.A., 2006. *Tectonic and metamorphic evolution of the north Qaidam ultrahigh- pressure metamorphic terrane, western China*. Ph.D. thesis. University of California, Los Angeles. 1–261.
- Menold, C.A., Manning, C.E., Yin, A., Tropper, P., Chen, X.H., and Wang, X.F., 2009. Metamorphic evolution, mineral chemistry and thermobarometry of orthogneiss hosting ultrahigh-pressure eclogites in the North Qaidam metamorphic belt, Western China. *Journal of Asian Earth Sciences*, 35: 273–284.
- Mo Xuanxue, Luo Zhaohua, Deng Jinfu, Yu Xuehui, Liu Chengdong, Chen Hongwei, Yuan Wanming, Liu Yunhua, 2007. Granitoids and crustal growth in the East-Kunlun orogenic belt. *Geological Journal of China Universities*, 13 (3): 403–414 (in Chinese with English abstract).
- Pan Yusheng, Xu Ronghua, Wang Dong'an, Zhou Weiming, Chen Ruijun, Zhang Yuquan, Xie Yingwen, Chen Ting'en, Luo Hui. 1998. The Caledonian structural belt and original Tethys in northern Qinghai-Tibet Plateau. In: Pan Yusheng and Kong Xiangru (eds.), *Lithosphere Structure, Evolution and Dynamics of Qinghai-Xizang (Tibetan) Plateau*. Guangzhou: Guangdong Science and Technology Press, 123–216 (in Chinese).
- Qin Jiangfeng, Lai Shaocong, Rodney Grapes, Diwu Chunrong, Ju Yinjuan and Li Yongfei, 2009. Geochemical evidence for origin of magma mixing for the Triassic monzonitic granite and its enclaves at Mishuling in the Qinling orogen (central China). *Lithos*, 112: 259–276.
- Qinghai Bureau of Geology and Mineral Resources (QBGM). 1991. *Regional Geology of Qinghai Province*. Geological Publishing House, Beijing. 1–662 (in Chinese with English abstract).
- Roger, F., Arnaud, N., Gilder, S., Tapponnier, P., Jolivet, M., Brunel, M., Malavieille, J., Xu, Z.Q., and Yang, J.S., 2003. Geochronological and geochemical constraints on Mesozoic suturing in east central Tibet. *Tectonics*, 22(4): 1037, doi:10.1029/2002TC001466.
- Song Yan, Zhao Menjun, Liu Shaobo, Hong Feng and Fang Shihu. 2010. Oil and gas accumulation in the foreland basins, central and western China. *Acta Geologica Sinica* (English Edition), 84 (2): 382–405.
- Stacey, J.S., and Kramers, J.D., 1975. Approximation of terrestrial lead isotope evolution by a two-stage model. *Earth and Planetary Science Letters*, 26: 207–221.
- Su Jianping, Hu Nenggao, Zhang Haifeng and Feng Beizhan, 2004. U-Pb zircon dating and genesis of the Heigouliangzi granitic intrusion in the western segment of the middle Qilian Mountains. *Geoscience*, 18 (1): 70–74 (in Chinese with English abstract).
- Sun Yangui, Zhang Guowei, Zheng Jiankang and Lu Xinxiang, 2001. Analysis of dynamic backgrounds of magmatic arc in the southeastern margin of Qaidam massif. *Geology and Mineral Resources of South China*, (4): 16–21 (in Chinese with English abstract).
- Tianjin Institute of Geology and Mineral Resources (TIGMR). 2004. *Report on Regional Geological Surveys of Dulan Sheet (1:250,000)*. Beijing: China Geological Survey, 1–385 (in Chinese).
- Wang Changgui and Lü Yousheng, 2004. Gonghe Basin: a new and worth-researching basin. *Xinjiang Petroleum Geology*, 25 (5): 471–473 (in Chinese with English abstract).
- Wang, E., and Burchfiel, B.C., 2004. Late Cenozoic right-lateral movement along the Wenquan fault and associated deformation: Implications for the kinematic history of the Qaidam Basin, northeastern Tibet Plateau. *International Geology Review*, 46: 861–879.
- Wang, G., Chen, N., Zhu, Y., and Zhang, K., 2003. Late Caledonian ductile thrusting deformation in the central East Kunlun belt, Qinghai, China and its significance: Evidence from geochronology. *Acta Geologica Sinica* (English edition), 77 (3): 311–319.
- Wu, C.L., Gao, Y.H., Wu, S.P., Chen, Q.L., Wooden, J.L., Mazadab, F.K., and Mattinson, C., 2007. Zircon SHRIMP U-Pb dating of granites from the Da Qaidam area in the north margin of Qaidam basin, NW China. *Acta Petrologica Sinica*, 23 (8): 1861–1875 (in Chinese with English abstract).
- Wu, C., Yang, J., Wooden, J.L., Shi, R., Chen, S., Meibom, A., and Mattinson, C., 2004a. Zircon U-Pb SHRIMP dating of the Yematan Batholith in Dulan, north Qaidam, NW China. *Chinese Sci. Bull.*, 49: 1736–1740.
- Wu Cailai, Yang Jingsui, Yang Hongyi, Wooden J, Shi Rendeng and Zheng Qiuguang, 2004b. Dating of two types of granite from north Qilian, China. *Acta Petrologica Sinica*, 20 (3): 425–432 (in Chinese with English abstract).
- Wu, C.L., Yang, J.S., Joseph, L.W., Liou, J.G., Li, H.B., Shi, R.D., Meng, F.C., Persing H., and Meibom, A., 2002. Zircon SHRIMP dating of granite from Qaidamshan, NW China. *Chinese Science Bulletin*, 47 (5): 418–422.
- Wu Cailai, Yang Jingsui, Ireland, T., Wooden, J., Li Haibing, Wan Yusheng and Shi Rendeng, 2001. Zircon SHRIMP ages of Aolaoshan granite from the south margin of Qilian shan and its geological significance. *Acta Petrologica Sinica*, 17 (2): 215–221 (in Chinese with English abstract).
- Wu Zhenhan, Hu Daogong, Song Biao and Zhou Chunjing, 2005. Ages and thermo-chronological evolution of the north Xidatan granite in the South Kunlun Mts. *Acta Geologica Sinica*, 79 (5): 628–635 (in Chinese with English abstract).
- Xu Zhiqin, Yang Jingsui, Wu Cailai, Li Haibing, Zhang Jianxin, Qi Xuexiang, Song Shuguang, Wan Yusheng, Chen Wen and Qiu Haijun. 2003. Timing and mechanism of formation and

- exhumation of the Qaidam ultrahigh pressure metamorphic belt. *Acta Geologica Sinica*, 77 (2): 163–176 (in Chinese with English abstract).
- Yang Jingsui, Xu Zhiqin, Song Shuguang, Zhang Jianxin, Wu Cailai, Shi Rendeng, Li Haibing, Brunel M. and Tapponnier P., 2002. Subduction of continental crust in the Early Palaeozoic North Qaidam ultrahigh-pressure metamorphic belt, NW China: Evidence from the discovery of coesite in the belt. *Acta Geologica Sinica (English Edition)*, 76 (1): 63–68.
- Yang Minghui and Song Jianjun. 2002. Petrology of the Lenghu granite mass, northwestern Qaidam Basin, China. *Northwestern Geology*, 35 (3): 94–98 (in Chinese with English abstract).
- Yin, A., and Harrison, T.M., 2000. Geologic evolution of the Himalayan-Tibetan orogen. *J. Annu. Rev. Earth Planet. Sci.*, 28: 211–280.
- Yin, A., Dang, Y.Q., Wang, L.C., Jiang, W.M., Zhou, S.P., Chen, X.H., Gehrels, G.E., and McRivette, M.W., 2008a. Cenozoic tectonic evolution of Qaidam basin and its surrounding regions (Part 1): The Southern Qilian Shan-Nan Shan thrust belt and northern Qaidam Basin. *Geological Society of America Bulletin*, 120: 813–846, DOI: 10.1130/B26180.1.
- Yin, A., Dang, Y., Zhang, M., Chen, X.H., and McRivette, M.W., 2008b. Cenozoic tectonic evolution of Qaidam Basin and its surrounding regions (Part 3): Structural geology, sedimentation, and regional tectonic reconstruction. *Geological Society of America Bulletin*, 120: 847–876, DOI: 10.1130/B26232.1.
- Yin An, Dang Yuqi, Zhang Min, McRivette, M.W., Burgess, W.P., and Chen, X., 2007. Cenozoic tectonic evolution of Qaidam basin and its surrounding regions (part 2): Wedge tectonics in southern Qaidam basin and the Eastern Kunlun Range. In: Sears, J.W., Harms, T.A., and Evenchick, C.A. (eds.), *Whence the Mountains? Inquiries into the Evolution of Orogenic Systems (A Volume in Honor of Raymond A)*. Price: Geological Society of America Special Paper, 433: 369–390, doi: 10.1130/2007.2433(18).
- Zhang Xueting, Yang Shengde and Yang Zhanjun. 2005. *Introduction to Regional Geology of Qinghai Province — Explanatory Notes of Geological Map of Qinghai Province in 1:1,000,000*. Beijing: Geological Publishing House. 1–158 (in Chinese with English abstract).
- Zheng Mianping, Zhang Yongsheng, Yuan Heran, Liu Xifang, Chen Wenxi and Li Jinsuo. 2011. Regional distribution and prospects of potash in China. *Acta Geologica Sinica (English Edition)*, 85 (1): 17–50.
- Zhong Jianhua, Wen Zhifeng, Guo Zeqing, Wang Haiqiao and Gao Jianbo, 2004. Paleogene and Early Neogene lacustrine reefs in the western Qaidam Basin, China. *Acta Geologica Sinica (English Edition)*, 78 (3): 736–743.

Paleozoic and Mesozoic Basement Magmatisms of Eastern Qaidam Basin, Northern Qinghai-Tibet Plateau: LA-ICP-MS Zircon U-Pb Geochronology and its Geological Significance



作者: [CHEN Xuanhua](#), [George GEHRELS](#), [YIN An](#), [LI Li](#), [JIANG Rongbao](#)
作者单位: [CHEN Xuanhua, LI Li, JIANG Rongbao \(Key Laboratory of Neotectonic Movement and Geohazard, Ministry of Land and Resources, Beijing 100081, China; Institute of Geomechanics, Chinese Academy of Geological Sciences, Beijing 100081, China\)](#), [George GEHRELS \(Department of Geosciences, University of Arizona, Tucson, AZ 85721, USA\)](#), [YIN An \(Department of Earth and Space Sciences, University of California, Los Angeles, CA 90095-1567, USA\)](#)

刊名: [地质学报 \(英文版\)](#) 
英文刊名: [Acta Geologica Sinica](#)
年, 卷(期): 2012, 86(2)

本文链接: http://d.g.wanfangdata.com.cn/Periodical_dzxb-e201202008.aspx